CONTINUUM FE MODELS FOR THE ANALYSIS OF MALLORCA CATHEDRAL

Pere Roca [a], Miguel Cervera [a], Luca Pelà [a *], Roberto Clemente [a]

[a] *Technical University of Catalonia (UPC), Campus Norte, Jordi Girona 1-3, 08034 Barcelona, Spain.*

Abstract – From the theoretical point of view, systems composed by masonry arches or vaults would require, during construction, the simultaneous activation of all structural elements in order to reach the optimum balance of thrusts. This is not obviously the case of complex ancient masonry constructions, whose long and gradual building process may have contributed to their deformed condition and even to damage.

In this paper, the possible influence of the construction process as well as that of later long-term deformation on the final condition of the building is investigated in the case of a complex and large historical structure, namely Mallorca Cathedral. A FE code has been specifically developed for the present study. The code is able to account for construction processes through sequential-evolutionary analyses, with the description of masonry mechanical damage and long-term deformation. A single typical bay of the cathedral is analysed taking into account different construction phases, as emerged from historical research. The response of such substructure to transverse earthquake equivalent forces is then investigated. In this case, the damage model is improved with a local crack-tracking algorithm. This numerical strategy models the tensile damage as distinct cracks, leading to a better prediction of realistic collapsing mechanisms.

Keywords: Historical Construction, Gothic Structure, Masonry, Construction Process, Long-term Effects, Continuum Damage Mechanics, Viscosity, Geometric Nonlinearity, Localized Damage, Crack-tracking.

* Corresponding author.

E-mail addresses: pere.roca.fabregat@upc.edu (Pere Roca), miguel.cervera@upc.edu (Miguel Cervera), luca.pela@upc.edu (Luca Pelà), clemente@cimne.upc.edu (Roberto Clemente).

1. Introduction

As recognized by relevant international documents [Iscarsah Recommendations, ISO13822], the study of large ancient structures is a multidisciplinary task requiring the integration of different activities such as historical investigation, experiments, structural analysis and monitoring. In particular, structural analysis is necessary to characterize the performance of the structure for a variety of actions, including gravitational loads, soil settlements, wind or earthquakes. Structural analysis of ancient masonry structures is carried out using a variety of tools, encompassing classical limit analysis and advanced numerical methods. Given the geometric and material complexity of many historical structures, their analysis has often resorted to computational tools involving up-to-date procedures for the modeling of the geometry and materials.

A variety of approaches has been proposed for the analysis of historical masonry structures. Classical limit analysis, as formulated by Heyman [1966] for arch structures, constitutes a powerful tool still in force. Advanced computational tools based on limit analysis have been proposed in [Orduña and Lourenço 2003, 2005; Gilbert et al. 2007] for blocky structures and in [Andreu et al. 2006; Block et al. 2006] for spatial systems and vaults. Nonlinear FE approaches have been proposed for the analysis of the whole structure [Pelà et al. 2009] or representative substructures [Genna et al. 1998, Pegon et al. 2001]. Several simplified approaches have been also formulated with the aim of approximating the macroscopic behaviour with reduced degrees of freedom [Molins and Roca 1998, Roca et al. 2005, Casolo and Sunjust 2009]. FEM based continuum mechanics models, where masonry is described as an equivalent orthotropic continuum using either plasticity or damage constitutive laws, have been proposed in [Papa 1996, Lourenço et al. 1998, Berto et al. 2002, Pelà et al. 2011]. Comparative studies carried out using different numerical strategies are reported in [Giordano et al. 2002, Mallardo et al. 2008]. A review of classical and advanced approaches for the analysis of historical masonry constructions can be found in [Roca et al. 2010].

As should be expected, actions and alterations occurred during the history of the building have often a significant impact on its present condition and existing damage. Due to it, studies on ancient buildings should take into account possible physical phenomena or significant damaging events having developed along the history of the building. Available information on historical events that have influenced on the structure should be considered in order to plan accurately the structural analyses and

interpret their results in a correct way. For that purpose, historical research, based on the investigation of historic documents, whenever available, constitutes an important complementary task to be undertaken in combination with structural analysis. Historical research is essential to provide information on relevant natural phenomena or anthropogenic alterations contributing to damage and deformation. It may also contribute with an understanding of the past-performance of the building after significant events, such as major earthquakes.

A phenomenon typically observed in many masonry historical buildings is their large deformed condition. In some cases, the amount of deformation far surpasses (by one or two orders of magnitude) predictions of numerical calculations assuming instant loading [Roca 2004]. The large deformation of historical structures is influenced by many historical factors that are not normally taken into account in the analyses, such as soil settlements, physical or chemical attack, long-term deformation of materials or multiple thermal cycles. Another contribution to deformation, and possibly to damage, can be found in the construction process itself. On the one hand, the construction influences the initial shape of the masonry structural members, due to deformation of centerings or to mortar settlement occurring after the removal of centerings. On the other hand, the construction may involve intermediate stages at which structural members or parts of them are led to resist in precarious or difficult equilibrium conditions. In particular, masonry buildings based on thrust equilibrium, as Gothic cathedrals, do not reach their optimal equilibrium condition until the completion of structure. During these intermediate stages, lasting in some cases for a long time, some parts of the buildings may have experienced significant initial deformation and even damage.

Another cause of deformation, damage and eventually collapse can be found in long term processes developing gradually across the history of the building. For instance, the effect of creep under constant stress, in the long term, may induce cumulative damage in rock-like materials [Binda, et al. 2001, 2003, Anzani et al. 2008]. The investigation of specimens cut from the walls of the Pavia Civic Tower after its collapse has suggested the possibility of failure due to long-term behaviour of the material. The identification of the problem has entailed some research effort to characterize better the phenomenon, and some models have been already proposed for its description [Lourenço and Pina-Henriques, 2008; Taliercio and Papa, 2008].

On the basis of the previous opening remarks, it emerges the need for enhanced analysis models, able to address the typical problems related to ancient structures, such as

deformations occurred during the construction process, historical architectural alterations, and long-term damage processes due to time-dependent phenomena developed along the life of the construction. Another fundamental issue is the formulation of reliable calculation tools for the seismic assessment of the historical constructions. Even when the monumental structures are located in low seismicity areas, their safety and preservation against exceptional events remains a matter of the greatest importance.

This paper presents a study on the possible influence of the construction process and the long term deformation on the present condition of an historical complex and large building, namely Mallorca Cathedral, situated in the city of Palma, Mallorca Island. The study is based on the information about the construction process and later architectural alterations obtained through detailed research by expert historians [Domenge 1997, 2003]. A numerical simulation of the construction process has been carried out by means of a sequential analysis, taking into account the main phases identified in the construction of the typical bay of the main nave. Long-term deformation has been then analysed by means of a viscoelastic model activated after the full completion of the bay. The analyses have been carried out using a continuum damage model. The study also includes the application of pushover analysis to estimate the seismic capacity of the structure in the transverse direction. For this latter analysis, a crack localization strategy has been utilized in order to obtain a more realistic description of damage.

A specific FE code has been elaborated in order to undertake the aforementioned analyses. The material viscous behaviour is modelled by a Maxwell's chain-type model [Cervera, 2003]. Mechanical damage is described by a tension-compression model characterized by two damage variables related to tensile and compressive stress states [Cervera et al. 1995, Faria et al. 1998]. The tensile crack localization is represented numerically by the crack-tracking algorithm proposed in [Cervera et al. 2010]. Although the FE tool has been devised specifically for the study of Mallorca Cathedral, it can be applied to other similar buildings in the field of the structural assessment and conservation of the architectural heritage.

2. Mallorca Cathedral

2.1 Description of the structure

The construction of the Cathedral of Santa Maria in Palma, island of Mallorca, Spain, started in year 1306 and spanned to year 1600 with a long interruption period from 1460

to 1560. The cathedral, with overall dimensions of 121 m in length and 55 m in width, is one of the most imposing Gothic buildings of the Mediterranean area (Figure 1). It presents typical formal features of the Catalan Gothic style, which derive from the search for a unique, spacious and diaphanous interior space. Typical features are the high lateral naves, the chapels between buttresses and the extremely slender octagonal piers, also present in the church of Santa Maria del Mar in Barcelona. In turn, the influence of northern Gothic can be found in the double battery of flying arches spanning over the aisles.

The cathedral dimensions are extraordinary. The central nave inner height of 44 m is only exceeded by Milan and Beauvais Cathedrals, while the free span of the high vaults, of 17.8 m, is only surpassed by that of Girona Cathedral, of 21.8 m. The height and width of the lateral naves are 29.4 m and 8.75 m, respectively. The nave vaults thickness is only 20 cm. The piers have an octagonal section with circumscribed diameter of 1.6 or 1.7 m and a height of 22.7 m to the springing of the lateral vaults. The piers slenderness, reaching a ratio of 14.2 between diameter and height, constitutes perhaps the more structurally daring aspect of the construction. In other Gothic cathedrals, this value normally stays between 7 and 9. The pier slenderness is counterbalanced by the very robust external buttresses, whose section is 7.7×1.5 m^2.

Two parts of the building can be distinguished from the plan and the sections shown in Figure 2. The first part, located towards the east, is the oldest one and includes the Royal Chapel (a single nave Gothic construction) and the Holy Trinity Chapel (the first element built in the complex). The second part is formed by the main nave and is subdivided, in turn, into three parallel naves separated by the very slender piers across eight bays, with the lateral chapels surrounding the buttresses.

The Cathedral is made of limestone masonry extracted from different local quarries. The piers were built using the more resistant limestone available in the island. The pillars section is solid and consists of four large hexagonal blocs surrounding an inner square one. The rest of the members, including vaults and buttresses, are built with comparatively poorer limestone. The lateral vaults are filled with lightweight pottery, whereas the central vaults do not show at present any filling except for the resistant backing at their lower regions. According to the historical research, the filling of the central vaults was probably removed during the 18th century, when for first time a tile roof was built over them to improve rainwater protection. As in other southern Gothic

cathedrals, the transverse arches of the main nave are diaphragmatic ones showing a solid spandrel wall over the ring.

A distinctive feature or Mallorca Cathedral is found in the large amount of dead weight laid over the transverse arches and central vault keystones (Figure 3). Pioneering studies based on graphic statics [Rubió, 1912] or photoelasticity [Mark 1984] already showed that this extra load was actually needed for a satisfactory equilibrium condition. A detailed overview of preliminary structural studies carried out on Mallorca Cathedral using both limit analysis and FE modelling are presented in [Roca 2004, Martínez 2007].

2.2 Present condition. Existing damage and deformation

In spite of some damage revealed by inspection, Mallorca cathedral shows mostly a satisfactory conservation condition. Maintenance works carried out throughout the history of the building and, particularly, major repairs undertaken during 18th c. and 19th c. have contributed to limit the extent of deterioration. In spite of it, damage and deformation can be seen in different parts of the building, as in particular in the piers, buttresses and flying arches (Figure 4). Some of these cracks have been repaired during recent restoration works.

Cracks affecting the clerestory walls of the western bay have been produced by a slight out-of-plumb experienced by the west façade. Some cracks are also visible in few piers. These cracks, seemingly caused by the compression forces, appear close to the corners (the less confined parts) of the octagonal section. In the case of one pier, these cracks were repaired in historical time and no reopening has occurred.

As mentioned, the deformation of the structure, and particularly that of piers and flying arches, is significant. The piers show remarkable curvature and lateral displacement especially along the direction transverse to the nave (Figures 5-6). Monitoring undertaken during the last years has shown that the deformation is now progressing at a very low rate. In particular, the maximum lateral deformation of piers is progressing at a ratio below 0.1 mm per year.

Both damage and deformation in piers appear in a rather random way with no systematic pattern. In particular, both the amount and direction of lateral deformation in piers are very variable (Figures 5-6). Maximum lateral displacement in piers ranges from 2 cm up to, in a single case, 26 cm, with an average (in absolute value) of 13 cm corresponding to a ratio of 1/115 with respect to the height.

Flying arches, and particularly those of the upper battery, show also significant deflection (Figure 4d). Part of this deformation may be due to the overall deformation of the structure and, particularly, to the outward rotation of flying arches. However, other non-mechanical effects may have as well contributed to this apparent deflection, among which the deformation of the centerings used during the construction and later loss of mortar in joints due to chemical problems. The mortar joints of flying arches had to be repeatedly repaired, as can be inferred from inspection and is also described in available historical documents.

A stone average compressive strength of 6 MPa was measured on samples taken in-situ from walls and buttresses, and a value of 28 MPa was obtained from samples of the quarries from which the material for the piers was taken. More information on damage and material deterioration can be found in [González et al. 2008]. In turn, information is provided in [Roca et al. 2008, Pérez-García et al. 2009] on the inspection works carried out on the building and the foundation soil, using different techniques.

From a structural point of view, the construction turns out to be an outstanding example of audacity in building. The great slenderness of the piers would seem daring even for a modern reinforced concrete element. The master builders definitely succeeded in designing highly optimized members, at least against the gravitational action. Dead loading does not appear as a cause for concern in the short term. However, a different scenario has to be considered in the long term as the continuous progression of deformation, in combination with geometric nonlinear effects, might compromise the stability of the structure. In addition, a seismic assessment of the building is considered necessary. Although the diaphragmatic transverse arches, the robust external buttresses and the use of light vault filling contribute in a favourable way to the seismic capacity, the structural features oriented to produce the diaphanous inner space (slender piers, large spans) add potential seismic weaknesses to the building.

2.3 Historical research

Historical research has been carried out through a detailed review of original documents available at the historical files of the library of the Chapter of the cathedral. These documents cover, with some unfortunate lacks, most of the period starting since the beginning of the construction to present. Research on these documents has provided significant hints on the construction process, later problems and historical repairs and reconstructions. It must be noted that most of the documents are mainly oriented to record accounting information on materials and wages, and additional interpretation is

needed as cooperation between historians and engineers. In a few cases, more technically oriented documents provide information on damage and historical repair operations.

Relevant information has been derived on construction sequence of the main nave in the progression in both the longitudinal and transverse directions. In the longitudinal direction the construction progressed, as in many other similar buildings, bay after bay from the presbytery towards the façade (the last part to be built). Construction of the chapels was ahead because of the funding provided by noble families or corporations willing them as pantheons or gremial chapels [Domenge, 1997].

It has been possible, at least for one of the bays (the 4th one starting from the east), to identify the sequence leading to its complete construction (Figure 7). Once again, it started with the lateral chapels, followed by the piers, then one lateral vault, then the other and finally the central one. In the case of this bay, the construction of the vaults lasted for 7 years, with some interruptions. The construction of each vault required about one year, and a period of 5 years elapsed between the completion of the first aisle vault and that of the central vault.

Historical investigation has also provided information on later problems and alterations. In fact, the building has experienced in the past significant problems and repairs. The 4th vault (previously discussed) partially collapsed 30 years after its construction. A significant number of vaults were repaired or reconstructed during the 17th, 18th and 19th centuries.

Regarding earthquake hazard, the Balearic Islands appear as a low seismicity place, compared to other Mediterranean areas. There is, however, historical information on different earthquakes having affected the city of Palma [Fontseré, 1918]. The only earthquake known to affect the cathedral was the one occurring in May 1851 (with estimated intensity between VII-VIII), causing damage to the façade and lateral towers. According to contemporary testimonies, no major damage appeared in the main structure of the building. The Renaissance façade of Mallorca Cathedral was dismantled in 1851 after the earthquake occurring during the same year. However, the decision on the demolition and rebuilding the façade had been already taken before the earthquake due to concern caused by its very large out-of-plumb (1.3 m). The original façade was replaced by the newly designed one, with more robust buttresses.

2.4 Hypothesis on the construction

The construction process described involves potential hazards on the stability at intermediate stages in both the longitudinal and transverse directions. In the longitudinal direction, the construction of one bay after the other causes a difficult condition due to the unbalanced longitudinal thrust that the lateral and central vaults apply on the piers. To avoid possible problems, auxiliary devices, such as iron ties or timber struts, may have been used in the construction of similar buildings. For instance, Viollet-le-Duc [1996] hypothesized for Medieval cathedrals the use of large-dimension timber shores transferring the thrust from the springing of vaults to the base of the piers of the following bay. In the case of Mallorca cathedral, the available documents do not provide any clue on the utilization of such devices, and no telltale of their use (such anchors, holes or receptacles) can be recognized in the fabric. As an alternative hypothesis, no auxiliary device might have been used, the master builders relying on the self-capacity of the vaults to keep stable during a limited period. Actually, this transitory stability might be possible thanks to a limited tensile strength of masonry. This tensile strength, normally not considered in the assessment of masonry structures, might be enough to keep the vault stable during a limited period, but is likely to vanish in the medium or long term due to environmental cyclic effects, wind, soil settlements and other causes.

A historical fact seems to confirm this possible understanding. The construction of the main nave was interrupted during one century after the erection of the 4th bay. As aforementioned, the central vault of this bay partially collapsed 30 years after its construction. The vault was rebuilt but collapsed again after another 30 years. The vault was rebuilt once more and the works were then continued until the full completion of the nave.

A similar problem appears in the transverse direction due to the construction of the lateral vaults prior to that of the central one. After the construction of the lateral vaults (Figure 7) a transverse unbalanced thrust is applied towards the piers. Again, the possibility of the structure enduring this condition without auxiliary devices for a limited period of time can be considered. Alternatively, the centering used for the main arches of the lateral vaults may have been left active until the construction of the central one. However, in ancient construction, centers would be normally eased to allow the work to set, which would in itself activate the vault. Even if the centerings were not eased, difficult equilibrium conditions would arise during their removal, causing

unbalanced inward or outward thrust depending of the order of the removal operation. All these hazards seem to be confirmed by the large variability of the lateral drift measured in the piers (Figures 5-6). Moreover, different approaches may have been used as well during the long construction process, adding to the variability of the lateral deformations detected across the bays. All this suggests that a significant part of the deformation may have appeared during the construction process and hence is not connected to later mechanical effects.

3. Model of analysis

The model adopted for the numerical analyses is based on Continuum Damage Mechanics theory. It includes the modelling of the phenomena considered relevant for the study of a representative Mallorca Cathedral's bay, such as mechanical damage and long-term viscous effects. The developed FE code is characterized by the possibility of carrying out sequential analyses in order to study the construction process. The damage model in tension has been further improved by means of a crack-tracking technique to describe tensile crack localization.

3.1 Viscoelasticity model

The viscoelasticity model proposed by Cervera [2003] is adopted in this work to account for masonry creep after the cathedral construction process, i.e. the time-dependent strain accumulation as a result of long-term exposure to applied stress. The approach adopted models the long-term deformation through a time-dependent stiffness, defined as the addition of a constant component and another susceptible to viscous relaxation.

The adopted rheological model can be schematized, for the uniaxial case, through the Maxwell chain shown in Figure 8a. The first chain element is composed of a spring with elastic stiffness E_∞, whereas the second element is composed of a spring with elastic stiffness E_v, arranged in series with a dashpot distinguished by a viscosity parameter η. Obviously, the springs response is linear elastic whereas the viscous stress in the dashpot is proportional to the viscous strain rate, i.e. $\sigma_v = \eta \dot{\varepsilon}_v$.

The initial stiffness of the system is given by the sum of the stiffnesses of the two springs, being the dashpot of the Maxwell chain infinitely stiff at the beginning of the deformation process. Thus, the instantaneous elastic modulus E can be defined as follows:

$$E = E_\infty + E_v \tag{1}$$

On the other hand, the stiffness of the system for $t = +\infty$ is equal to E_∞, since the dashpot is completely slackened at the end of the deformation process.

The total stress sustained by the Maxwell chain is given by the sum of the stresses in the two elements,

$$\sigma = E_\infty \varepsilon + \xi E\left(\varepsilon - \varepsilon_v\right) \tag{2}$$

where $\xi = E_v / E$ is the participation ratio which denotes the amount of stiffness susceptible to viscosity. The total deformation of the system is denoted by ε, whereas ε_v denotes the viscous strain of the chain which increases with time under a constant stress σ. The phenomenological behaviour of the model is depicted in Figures 8b-d, which also stress the effect of the so-called retardation time $\vartheta = \eta / E_v$ on the time-dependent increase of strain or decrease of stiffness.

The strain rate of the system is defined by the following equation:

$$\dot{\varepsilon} = \frac{\dot{\sigma}_v}{E_v} + \frac{\sigma_v}{\eta} \tag{3}$$

The previous equation can be rewritten for the multidimensional case, using the tensorial counterparts of the scalar terms used for the uniaxial model and making reference to the two parameters of the model ξ and ϑ:

$$\xi \mathbf{C} : \dot{\boldsymbol{\varepsilon}} = \dot{\boldsymbol{\sigma}}_v + \frac{\boldsymbol{\sigma}_v}{\vartheta} \tag{4}$$

where $\mathbf{C}$ is the elastic tensor. With the aim of assuming the viscous strain in the Maxwell chain as internal variable, the relationship

$$\boldsymbol{\sigma}_v = \xi \mathbf{C} : \left(\boldsymbol{\varepsilon} - \boldsymbol{\varepsilon}_v\right) \tag{5}$$

can be included in Equation (4), leading finally to the evolution law for the viscous strain:

$$\dot{\boldsymbol{\varepsilon}}_v = \frac{1}{\vartheta}\left(\boldsymbol{\varepsilon} - \boldsymbol{\varepsilon}_v\right) \tag{6}$$

The solution of the differential equation for a generic time step t_{n+1} can be obtained by integrating the previous equation, leading finally to [Cervera, 2003]

$$\boldsymbol{\varepsilon}_v\left(t_{n+1}\right)=\boldsymbol{\varepsilon}_v\left(t_n\right)+\frac{\Delta t}{\vartheta}\left[\boldsymbol{\varepsilon}\left(t_{n+1}\right)-\boldsymbol{\varepsilon}_v\left(t_n\right)\right] \tag{7}$$

3.2 Tension-compression damage model

The mechanical damage in masonry due to cracking and crushing is described by the Tension-Compression Damage Model [Cervera et al. 1995, Faria et al. 1998], which is based on the concept of effective stress tensor $\bar{\boldsymbol{\sigma}}$ related to strains $\boldsymbol{\varepsilon}$ under elastic regimen:

$$\bar{\boldsymbol{\sigma}}=\mathbf{C}:\boldsymbol{\varepsilon} \tag{8}$$

where $\mathbf{C}$ is the isotropic linear-elastic constitutive tensor. In order to account for the different mechanical behaviour in tension and compression, a split of the effective stress tensor into tensile and compressive components, $\bar{\boldsymbol{\sigma}}^{+}$ and $\bar{\boldsymbol{\sigma}}^{-}$, is introduced according to:

$$\bar{\boldsymbol{\sigma}}^{+}=\sum_{i=1}^{3}\left\langle\bar{\sigma}_i\right\rangle \mathbf{p}_i\otimes\ \mathbf{p}_i \quad \text{and} \quad \bar{\boldsymbol{\sigma}}^{-}=\bar{\boldsymbol{\sigma}}-\bar{\boldsymbol{\sigma}}^{+} \tag{9}$$

where $\bar{\sigma}_i$ denotes the *i*-th principal stress value from tensor $\bar{\boldsymbol{\sigma}}$, $\mathbf{p}_i$ represents the unit vector associated with its respective principal direction and the symbols $\langle . \rangle$ are the Macaulay brackets $\left(\langle x\rangle = x,\ if\ x\geq 0, \langle x\rangle = 0,\ if\ x<0\right)$.

Once defined the internal damage variables d^{+} and d^{-}, each related with the sign of the stress and thus with tension and compression, the constitutive equation takes the form:

$$\boldsymbol{\sigma}=\left(1-d^{+}\right)\bar{\boldsymbol{\sigma}}^{+}+\left(1-d^{-}\right)\bar{\boldsymbol{\sigma}}^{-} \tag{10}$$

The internal damage variables are equal to zero when the material is undamaged and equal to one when it is completely damaged.

Different damage criteria are assumed for tension and compression stress states in order to describe different failure mechanisms for masonry, i.e. cracking and crushing of the material. The damage functions are defined as:

$$\Phi^{\pm}\left(\tau^{\pm}, r^{\pm}\right)=\tau^{\pm}-r^{\pm}\leq 0 \tag{11}$$

being $\tau^{\pm}$ scalar positive quantities, termed as equivalent stresses and defined in order to compare different stress states in two- or three-dimensions:

$$\tau^{\pm}=\left[\bar{\boldsymbol{\sigma}}^{\pm}:\boldsymbol{\Lambda}^{\pm}:\bar{\boldsymbol{\sigma}}^{\pm}\right]^{1/2} \tag{12}$$

The shape of each damage criterion is defined by tensors $\mathbf{\Lambda}^{\pm}$. In this work, for the particular case of masonry material, it is assumed that $\mathbf{\Lambda}^{+} = \mathbf{p}_1 \otimes \mathbf{p}_1 \otimes \mathbf{p}_1 \otimes \mathbf{p}_1$, which corresponds to the Rankine criterion in tension, while for the compression case it is assumed that $\mathbf{\Lambda}^{-} = \mathbf{C}/E$, where E is the Young's modulus. Figure 9 shows the resulting representation of the composite damage criterion for the two-dimensional case.

Variables $r^{\pm}$ are internal stress-like variables representing the current damage threshold and their values control the size of the (monotonically) expanding damage surface. The initial values of the damage thresholds are $r_0^{\pm} = f^{\pm}$, where f^{+} and f^{-} are the uniaxial strengths in tension and compression. The evolution law of the internal variables $r^{\pm}$ is explicitly defined in the following way:

$$r^{\pm} = \max\left[r_0^{\pm}, \max\left(\tau^{\pm} \right) \right] \tag{13}$$

Finally, the damage indexes $d^{\pm}$ are defined in terms of the corresponding current value of the damage thresholds $r^{\pm}$ in the form of a monotonically increasing function such that $0 \le d^{\pm}\left(r^{\pm}\right) \le 1$. In this work, the following exponential expressions are assumed

$$d^{\pm}\left(r^{\pm}\right) = 1 - \frac{r_0^{\pm}}{r^{\pm}} \exp\left\{ 2\, H_{dis}^{\pm} \left(\frac{r_0^{\pm} - r^{\pm}}{r_0^{\pm}} \right) \right\} \tag{14}$$

where constants $H_{dis}^{\pm} \ge 0$ are the discrete softening parameters [Cervera et al. 2010]. They are related to material tensile and compressive fracture energies $G_f^{\pm}$, normalized according to the finite element characteristic length, in order to ensure objectivity of the FEM solution respect to the mesh size [Cervera et al., 1987].

It is worth noticing that more sophisticated damage models could be adopted, including also the description of different stiffnesses, strengths and inelastic responses along the different material axes [Pelà et al. 2011]. The choice of a simpler model for this study is due to lack, at the moment, of available experimental tests concerning the orthotropic properties of the masonries of the building.

3.3 FE activation technique for sequential analysis

An accurate simulation of the construction process of a historical construction may be very difficult, if feasible at all, due to lack of information on the real sequences and structural responses corresponding to each construction phase. Even if some insight on the construction phases can be obtained, as in the case of Mallorca cathedral, no direct

information will normally be possible on the real initial shapes of the parts subsequently added during the entire process. On the one hand, as mentioned, these shapes were influenced by the deformation of centerings, mortar settlement and possible initial soil-settlements. On the other hand, the shape of the parts subsequently added did not fully correspond to the original drawings or intentions, but was gradually corrected to meet the deformed shape of the already built ones. A true simulation according to all these considerations is not possible for obvious reasons.

In spite of these difficulties, an attempt has been made to analyse, in a simplified way, the possible response of the intermediate construction stages and its possible impact on the overall deformation. The strategy considered for this purpose uses a unique FE mesh for the entire construction and introduces some opportune corrections to account for the deformation of parts already built.

The simulation of the construction process according to this approach requires, from the numerical point of view, an ad hoc finite element activation technology able to reproduce the addition of different structure portions during the building stages. This method classifies the elements of the overall FE mesh into active and inactive. At the beginning of the analysis, the elements which define the first portion built are activated, i.e. computed and assembled into the global matrix, whereas the inactive elements are disregarded in calculations. In the following step, the elements corresponding to the next construction stage are activated and the calculation proceeds, considering the first portion already deformed. However, the activation of each phase requires the previous updating of the corresponding mesh portion, in order to account for the movements of the portions corresponding to the previous phases. This correction is of particular importance when nonlinear geometric effects are taken into account. In this work, this updating is carried out by considering the following assumptions:

(1) Horizontal and vertical lines maintain their direction. Actually, historic builders would have corrected any rotation in these lines caused by deformation of previous phases.

(2) The total elongation of the line at the boundary between parts corresponding to different phases is negligible. Therefore, no dimensional correction is necessary on the mesh corresponding to the new phase and the updating can be performed as a rigid body translation.

These hypotheses allow for a very direct approach. Given a previous, already deformed phase and a new phase to be activated, a vector $\boldsymbol{u_d}$ is firstly computed as the average

displacement vector of the nodes in the boundary of the two phases (nodes *i*, *j*, *k* of Figures 10a-b). The rest of the nodes corresponding to the new phase are then updated according to the translation defined by vector $\boldsymbol{u_d}$ (Figure 10c). Because of this translation, the elements of the new part located close to the boundary experience a change in their shape and hence an initial strain which must be evaluated, stored and discarded in the computation of the stresses in those elements at subsequent times.

An important advantage of the proposed activation technique is the possibility of defining the computational mesh independently of the construction process. Different hypotheses about the building stages can be considered by simply changing the activation sequence or the grouping of elements. This is very useful in case of historical constructions, where comparative studies are often necessary in order to assess the most critical construction process that might be experienced by the structure.

3.4 Crack-tracking technique for localized damage

The classical smeared crack approach, based on standard finite elements and Continuum Damage Mechanics models, such as the one presented in Section 3.2, provides an approximate representation of the damaging process occurring on the material. This is more evident in case of tensile damage, which is portrayed as a spreading phenomenon involving large regions of the construction. This approach is not very satisfactory in the case of unreinforced masonry construction, where damage normally appears in the form of large individual cracks.

This limitation is overcome in this work adopting the crack-tracking technique proposed in [Cervera et al. 2010], which forces the tensile crack to develop along a single row of finite elements according to the direction of the main tensile stress. The generation of these localized cracks represents more realistically the behaviour of the structure in the ultimate condition [Cervera and Chiumenti 2006a-b].

The proposed method is applied at every time step during the FE analysis, just before the stress evaluation. The algorithm is able to detect the point of the boundary of the structure where a crack is originated. Making use of a flag system, finite elements are then labelled to delimit the zones where cracks will appear or develop. The criteria used to define these zones depend on the magnitude and direction of the principal stresses at each element. A minimum distance between two crack root elements, called exclusion radius, is used to guarantee the creation of separated discrete cracks. More specifically, the exclusion radius is defined as the minimum distance imposed between two crack

root elements. The algorithm ensures mesh-bias and element-size objective FE results and has been implemented for 2D problems using three-noded triangular elements.

4. Structural analyses

The viscoelasticity and tension-compression models, the FE activation strategy and the crack-tracking techniques presented in Section 3 have been implemented into the FE program COMET [2002] developed at the International Centre for Numerical Methods in Engineering (CIMNE, Barcelona). It is worth pointing out that this enhanced FE package has been devised exclusively for the numerical analysis of Mallorca Cathedral. The obtained results are summarized in this Section. Pre- and post-processing have been carried out with GiD [2002], also developed at CIMNE.

4.1 Sequential analysis for construction process simulation

The analysis of a single typical bay has been carried out on a structural model including piers, buttresses, flying arches, nave vaults and aisles (Figure 11a). Such macroelement has been considered as the most representative for the purpose of investigating the possible link between construction process and existing deformation. Due to symmetry of geometry and load, a three-dimensional FE model has been elaborated representing only a quarter of the typical bay (Figure 11b). Appropriate boundary conditions have been considered in order to account for symmetry and the effect of the adjacent bays. The adopted FE mesh is composed by 49,979 tetrahedral elements and 14,689 nodes. Mesh refinement has been carried out in zones where high stress gradients are expected, as at both ends of flying arches and columns, at the intersection between different structural elements and under the large false window located in buttresses.

The different structural members have been modelled using the results of the in-field survey. Piers are solid, buttresses and walls are defined as three-leaf or solid members. Conservatively, the false window existing in the buttresses, characterized by a reduced thickness, has been modelled as a real opening. Non-resisting elements such as pinnacles, infills and stone pyramids over the vaults have not been included in the model, but by the weight that they apply on the rest of the structure.

Three materials have been distinguished with different parameters, see Table 1. Masonry compressive strength has been estimated based on previous experience for similar materials. The tensile strength has been assumed equal to 5% of the compressive strength. The Young moduli have been assessed making reference to the structural identification procedure reported in [Martínez, 2007]. Values for the fracture energies

have been assumed based on previous experience, since they were not measured experimentally.

In compliance with the information about the building stages provided by the historical investigation, the numerical simulation of the construction process consists of three subsequent analysis steps. In the first step, only the lower part of the FE model is activated, making use of the technique explained in Section 3.3, including the pier, the aisle vault and the buttress. In the second analysis step, the upper part of the FE model is subsequently activated (i.e. the upper part of the buttress, the flying arches, the clerestory, the nave vault) and the computation is carried on starting from the stress-strain state obtained at the end of first analysis. Finally, the structure is subject to constant loading and the time starts elapsing in order to evaluate the deformation accumulation due to creep.

The numerical simulation results of the first construction stage are represented in Figures 12a-b, in terms of deformed shape and tensile damage. The resulting deformation at the top of the pier is equal to 3 cm. At that location, at the side towards the central nave, tensile damage occurs and also at the key of the aisle vault, at the transverse rib and at the bottom of the large window located in buttresses. Such amount of damage is actually greater than that observed on the real structure. However, the numerical analysis clearly shows that such partial configuration of the bay is stable, pointing to the possibility of the bay having been built following the supposed construction process.

The deformed shape and the tensile damage contour after the second construction stage are represented in Figures 12c-d. The maximum lateral displacement at the pier decreases to 1.8 cm due to thrust exercised by the central vault. As in the previous analysis step, the compressive damage does not affect any structural member in a significant way.

4.2 Simulation of long-term deformation

The analysis of the long-term deformation is carried out on the configuration resulting from the previous construction process simulation. Although the possible viscous deformation experienced in-between the construction phases might be meaningful, the analysis focuses in the deformation accumulation occurring after the completion of the bay.

The evaluation of time-dependent deformation due to creep requires the definition of two parameters, i.e. the retardation time ϑ and the participation ratio ξ, in compliance with the viscoelasticity model proposed in Section 3.1.

For obvious reasons, it is difficult to identify and simulate in an accurate way the real long-term deformation trends experienced by an historical building across its lifetime. The viscoelastic model adopted, however, permits an investigation on the joint influence of long term deformation and geometric nonlinear effects on the stability of the building. For this purpose, the time is measured in "pseudo-time" units without fixed quantitative relationship with real time and no attempt is made to relate it with the true pace of deformation increase in historic time. The retardation time is assumed arbitrarily as $\vartheta = 50$ time units. In the present analysis, its effective entity is not significant and has to be related only to the total number of time steps in calculations. Concerning the participation ratio, two different values, $\xi = 0.875$ and $\xi = 0.975$, producing very different results, have been considered. These assumed values are large enough to analyse the structure under adverse conditions, since they presume that a significant amount of stiffness is susceptible to creep. In this way, the possible influence of long-term deformation on the structure can be studied, even if its real participation ratio in the historical time is not known.

Figure 13a shows the maximum horizontal displacements increase at pier top due to creep, corresponding to the two assumed values of participation ratio, in the case of geometric linear analysis. Three points are highlighted in each curve; points 1-2 denote the pier top horizontal displacement after the first and second construction stage, whereas point 3 is the final displacement due to creep obtained at the end of the simulation. For $\xi = 0.875$, the time-dependent displacement reaches a stable value after 1,000 time units, whereas for $\xi = 0.975$ this condition is achieved after 2,000 time units. The tendency of the time-dependent displacement to stabilize is given by the nature of the considered constitutive model and the hypothesis of geometric linearity. It is worth noticing that although the displacements increase under creep phenomenon, the tensile damage distribution remains similar to the one depicted in Figure 12d, since creep does not alter the stress state of the structure under the hypothesis of geometric linearity.

A similar study has been repeated for nonlinear geometric analysis through a total Lagrangian formulation with the assumption of small-strain/large-displacement. Figure 13b shows the corresponding horizontal displacements evolution at pier top due to

creep. The displacement values result considerably higher than in case of geometric linearity (Figure 13a), showing the large influence of the deformation of piers in the equilibrium condition of the structure. In addition, the two assumed values of the participation ratio lead to completely different results. In case of $\xi = 0.875$, the pier maximum horizontal time-dependent displacement reaches a stable value of 12 cm after 3,000 time units. This order of magnitude is comparable to the average displacements actually observed in Mallorca Cathedral bays (Figure 6), showing that the combination of long-term deformation and non-linear geometric effects may have played a significant role during the life of the structure. It is worth noticing that a conventional instantaneous analysis of the cathedral bay, i.e. without considering the construction process simulation with viscoelasticity model and geometric nonlinearity, would have led erroneously to a horizontal displacement at the pier top of only 0.76 cm.

The assumption of $\xi = 0.975$ in the frame of a nonlinear geometric analysis leads to the instability of the structure at 2,000 time units, as shown by the corresponding curve in Figure 13b. It can be concluded that the numerical simulation can represent the failure condition only for extremely high values of the participation ratio. However, such very high values might be realistic for very long historical periods, during which creep might acquire a low diminishing rate or even develop at an almost constant rate (secondary creep).

Finally, Figures 14a-b show the deformed shape and the tensile damage contour at the end of the sequential analysis with geometric nonlinearity for $\xi = 0.875$ and, $\xi = 0.975$, respectively. A careful comparison with Figures 12c-d, related to the end of the second construction stage, shows clearly how displacements increase and tensile damage propagates due to combined effect of long-term deformation and geometric non-linearity. Figure 14b shows the condition of the structure prior to failure for $\xi = 0.975$, with significant damage accumulated at the aisle vault, the pier and the flying arches.

4.3 Seismic Load Analysis

The typical bay seismic performance has been assessed by means of a pushover analysis consisting of the gradual application of a system of lateral equivalent static forces on the structure. The analysis has been carried out resorting to an enhanced continuum damage model able to describe tensile crack localization through the crack-tracking technique discussed in Section 3.4. Since such numerical tool is implemented for two-dimensional problems, the analysis is in this case carried out on a plane-stress FE model. This model

has been calibrated by ensuring that the weight of all members is equal to the corresponding one in the three-dimensional model. Moreover, the thickness of different components has been modified in such a manner that the two-dimensional and the three-dimensional FE models present equivalent deformed shapes after a linear elastic analysis. The thicknesses of the different structural elements in the two-dimensional FE model are summarizes in Table 2. The entire bay structure has been discretized by a FE mesh composed by 32,858 triangular elements and 17,628 nodes, see Figure 15. Two loading conditions have been applied in consecutive phases. The gravity load is applied in the first step. In the second step the lateral forces proportional to mass distribution are applied and increased gradually until reaching failure.

Different analyses have been carried out considering three different values for the exclusion radius r_{excl}, in order to investigate their influence on results; the values adopted are 1 m, 2 m and 3 m. The lowest value of r_{excl} that has been assumed in the analyses corresponds approximately to the dimension of a stone unit.

Figure 16 shows the seismic load multiplier (defined as a fraction of gravity acceleration) against the horizontal displacement at the top of the piers. The smeared damage model causes failure for a load factor of about 0.08. The localized damage model produces a higher failure load factor, ranging between 0.1 for $r_{excl} = 1\,\mathrm{m}$ and 0.12 for $r_{excl} = 3\,\mathrm{m}$, as expected due to restrictions that the model imposes to the formation and propagation of damage. It is worth noticing that such seismic load multipliers are similar to the design values that can be determined from the Spanish seismic provisions NCSE-02 [2002] for the location of the cathedral with a return period of 1000 years.

Figure 17 depicts the deformations and the tensile damage distribution obtained by the analyses with smeared damage model and localized damage model. The latter model affords a more realistic representation of the possible location and extent of the tensile cracks, allowing a better understanding of the real collapse mechanism under seismic loading. The more damage portions are the base of columns and buttresses, the vaults and the flying arches. The presence of the big false windows contributes to weaken the buttresses by facilitating the generation of a large crack in them.

5. Conclusions

A specific FE tool has been prepared to analyse large historical masonry constructions, taking into account sequential-evolutionary processes, such as the construction phases,

and later long-term deformation phenomena. The evolutionary processes are simulated by means of a simplified approach for sequential analysis, while the influence of the long term deformation is modelled using a viscoelastic model in the frame of non-linear geometric analysis. The mechanical damage propagation is described by means of a continuum damage model.

The FE code has been successfully used to investigate the influence of construction and later deformation in the long term on a substructure of a large and complex masonry historical building. As exemplified by the case of Mallorca Cathedral, the construction processes, having to overcome difficult intermediate phases, may have in some cases contributed meaningfully to the deformation and even to the damage of historic structures. Later long-term processes related to creep and other phenomena may have expanded significantly the deformed condition while also generating damage and even stability problems due to activation of non-linear geometric effects.

In the case of Mallorca Cathedral, and according to the present study, significant further progress of the lateral deformation of the pier might bring stability problems. Also according to the present study, the building is at present far from this concerning condition. However, monitoring, already in progress, is considered convenient to identify the deformation trends and characterize the safety condition of the building in the medium and the long-term.

The response of the typical bay structure to transverse earthquake static equivalent forces has been also investigated making use of an enhanced damage model able to describe tensile crack localization through a crack-tracking technique. The crack-tracking model has enabled the simulation of more realistic damage distribution and failure mode compared to the smeared damage approach, without requiring significant additional computation cost.

6. Acknowledgments

The studies presented here have been developed within the research project SEDUREC (CSD2006-00060), funded by DGE of the Spanish Ministry of Science and Technology, and project NIKER (contract agreement 244123) funded by the 7th Frame Programme of the European Union, whose assistance is gratefully acknowledged.

7. References

[1] ICOMOS / ISCARSAH Committee. ICOMOS Charter – Principles for the analysis, conservation and structural restoration of architectural heritage; 2003. http://iscarsah.icomos.org/content/principles/ISCARSAH_Principles_English.pdf

[2] ISO/TC98. ISO/FDIS 13822 Bases for design of structures – Assessment of existing structures. Genève: ISO; 2010.

[3] Heyman J. The stone skeleton. Int J Solids Struct 1966;2:270-79.

[4] Orduña A, Lourenço PB. (2003). Cap model for limit analysis and strengthening of masonry structures. J Struct Eng 2003;129:1367–1375.

[5] Orduña A, Lourenço PB. Three-dimensional limit analysis of rigid block assemblages. Part I: Torsion failure on frictional interfaces and limit analysis formulation. Int J Solids Struct 2005;42:5140–5160.

[6] Gilbert M, Casapulla C, Ahmed HM. Limit analysis of masonry block structures with non-associative frictional joints using linear programming. Comput Struct 2006;84:873-887.

[7] Andreu A, Gil L, Roca P. Computational analysis of masonry structures with a funicular model. J Eng Mech, 2007;133(4):473–480.

[8] Block P, Ciblac T, Ochsendorf JA. Real-Time Limit Analysis of Vaulted Masonry Buildings. Comput Struct 2006;84:1841–1852.

[9] Pelà L, Aprile A, Benedetti A. Seismic assessment of masonry arch bridges. Eng Struct 2009;31(8):1777-1788.

[10] Genna F, Di Pasqua M, Veroli M. Numerical analysis of old masonry buildings: A comparison among constitutive models. Eng Struct 1998;20:37–53.

[11] Pegon P, Pinto AV, Géradin M. Numerical modelling of stone-block monumental structures. Comput Struct 2001;79:2165-2181.

[12] Molins C, Roca P. Capacity of masonry arches and spatial frames. J Struct Eng 1998;124(6):653–663.

[13] Roca P, Molins C, Marí AR. Strength capacity of masonry wall structures by the equivalent frame method. J Struct Eng 2005;131(10):1601–1610.

[14] Casolo S, Sanjust CA. Seismic analysis and strengthening design of a masonry monument by a rigid body spring model: the “Maniace Castle” of Syracuse. Eng Struct 2009;31:1447–1459.

[15] Papa EA. Unilateral damage model for masonry based on a homogenization procedure. Mech Cohes-Frict Mat 1996;1:349-366.

[16] Lourenço PB, Rots JG, Blaauwendraad J. Continuum model for masonry: Parameter Estimation and Validation. J Struct Eng 1998;1(6);642-652.

[17] Berto L, Saetta A, Scotta R, Vitaliani R. An orthotropic damage model for masonry structures. Int J Numer Methods Eng 2002;55:127-157.

[18] Pelà L, Cervera M, Roca P. Continuum damage model for orthotropic materials: application to masonry. Comput Methods Appl Mech Eng 2011;200:917-930.

[19] Giordano A, Mele E, De Luca A. Modelling of historical masonry structures: Comparison of different approaches through a case study. Eng Struct 2002;24:1057–69.

[20] Mallardo V, Malvezzi R, Milani E, Milani G. Seismic vulnerability of historical masonry buildings: a case study in Ferrara. Eng Struct 2008;30:2223–2241.

[21] Roca P, Cervera M, Gariup G, Pelà L. Structural Analysis of Masonry Historical Constructions. Classical and Advanced Approaches. Arch Comput Methods Eng 2010;17:299–325.

[22] Roca P. Considerations on the significance of history for the structural analysis of ancient constructions. In: Modena C, Lourenço PB, Roca P, editors. Structural analysis of historical constructions IV. Padova; 2004, p. 63–73.

[23] Binda L, Saisi A, Messina S, Tringali S. (2001). Mechanical damage due to long term behaviour of multiple leaf pillars in Sicilian churches. In: Lourenço PB, Roca P, editors. III International Seminar: Historical Constructions. Possibilities of Numerical and Experimental Techniques. Guimaraes; 2001, p. 707-718.

[24] Binda L, Anzani A, Saisi A. Failure due to long term behaviour of heavy structures: the Pavia Civic Tower and the Noto Cathedral. 8th Int. Conf. on STREMAH 2003, Structural Studies Repairs and Maintenance of Heritage Architecture. Halkidiki; 2003, p. 99-108.

[25] Anzani A, Binda L, Mirabella-Roberti G. (2008) Experimental researches into long-term behavior of historical masonry. In: Binda L, editor. Learning from failure: long term behaviour of heavy masonry structures. Southampton: WIT Press; 2008.

[26] Lourenço PB, Pina-Henriques J. (2008) Collapse prediction and creep effects. In: Binda L, editor. Learning from failure: long term behaviour of heavy masonry structures. Southampton: WIT Press; 2008.

[27] Taliercio A, Papa E. (2008) Modelling of the long-term behavior of historical towers. In: Binda L, editor. Learning from failure: long term behaviour of heavy masonry structures. Southampton: WIT Press; 2008.

[28] Domenge J. The construction process of Mallorca cathedral in 300 years (in Catalan). Palma de Mallorca; 1997.

[29] Domenge J. Study of the Cathedral historical books (in Spanish), Document No. 3. Estudio, diagnóstico y peritación y en su caso planteamiento de actuaciones sobre el comportamiento constructivo-estructural de la catedral de Santa María, en la ciudad de Palma, isla de Mallorca (Baleares). Fase primera. Barcelona: Technical University of Catalonia; 2003.

[30] Cervera M. Viscoelasticity and rate-dependent continuum damage models. Monography No-79. Barcelona: CIMNE, Technical University of Catalonia; 2003.

[31] Cervera M, Oliver J, Faria R. Seismic evaluation of concrete dams via continuum damage models. Earthq Eng Struct D 1995;24(9):1225–1245.

[32] Faria R, Oliver J, Cervera M. A strain-based plastic viscous-damage model for massive concrete structures, Int J Solids Struct 1998;35:1533–1558.

[33] Cervera M, Pelà L, Clemente R, Roca P. A crack-tracking technique for localized damage in quasi-brittle materials. Eng Fract Mech 2010;77(13):2431-2450.

[34] Rubió J. Conferencia acerca de los conceptos orgánicos, mecánicos y constructivos de la catedral de Mallorca (in Spanish). Anuario de la Asociación de Arquitectos de Cataluña. Barcelona; 1912.

[35] Mark R. Experiments in Gothic Cathedrals. Cambridge: MIT Press; 1984.

[36] Roca, P. Description of Mallorca cathedral. Report of project Improving the Seismic Resistance of Cultural Heritage Buildings, EU-India Cross Cultural Programme. Barcelona: Technical University of Catalonia; 2004.

[37] Martínez G. Seismic vulnerability of masonry long and medium span historical buildings (in Spanish). Ph.D. Thesis. Barcelona: Technical University of Catalonia; 2007.

[38] González R, Caballé F, Domenge J, Vendrell M, Giráldez P, Roca P, González JL. Construction process, damage and structural analysis. Two case studies. In: D'Ayala and Fodde, editors. Structural Analysis of Historic Construction: Preserving Safety and Significance. Bath; 2008, p. 643-651.

[39] Roca P, Clapés J, Caselles O, Vendrell M, Giráldez P, Sánchez-Beitia S. Contribution of inspection techniques to the assessment of historical structures. Proceedings of the International RILEM SACoMaTiS Conference. Varenna; 2008.

[40] Pérez-Gracia V, Caselles JO, Clapes J, Osorio R, Martínez G, Canas JA. Integrated near-surface geophysical survey of the Cathedral of Mallorca. J Archaeol Sci 2009;36:1289–1299.

[41] Fontseré E. Recopilació de dades sísmiques de les terres catalanes entre 1100 i 1906 (in Catalan). Barcelona: Fundació Salvador Vives Casajuana; 1971.

[42] Viollet-le-Duc E. The Medieval construction (in Spanish). In: Huerta S., editor. Madrid: Instituto Juan de Herrera; 1996. Translation to Spanish from the French original of the article on "Construction" of the Dictionnaire Raisonnée de l'architecture française du XIe au XVI siècles.

[43] Cervera M., Hinton E., Hassan O. Non linear analysis of reinforced concrete plate and shell structures using 20-noded isoparametric brick elements. Comput Struct 1987; 25(6):845-869.

[44] Cervera M, Chiumenti M. Smeared crack approach: back to the original track. Int J Numer Anal Methods Geomech 2006; 30:1173–1199.

[45] Cervera M, Chiumenti M. Mesh objective tensile cracking via a local continuum damage model and a crack tracking technique. Comput Methods Appl Mech Eng 2006; 196:304–320.

[46] Cervera M, Agelet de Saracibar C, Chiumenti M. COMET: COupled MEchanical and thermal analysis – data input manual version 5.0. Technical report IT-308. Barcelona: CIMNE, Technical University of Catalonia; 2002.

[47] GiD: the personal pre and post-processor. Barcelona: CIMNE, Technical University of Catalonia; 2002. http://gid.cimne.upc.es

[48] Comisión Permanente de Normas Sismoresistentes, General code for seismic resistant construction (in Spanish), Real Decreto 997/2002. Madrid: Spanish Ministry of Public Works; 2002.

8. Table Captions

Table 1 Material parameters adopted in numerical analyses.

Table 2 Thicknesses of different components in the two-dimensional FE model.

9. Figure Captions

Figure 1 Mallorca Cathedral: external view (a) and view from the interior (b).

Figure 2 Plan at roof level (a), transverse section (b), longitudinal section (c) and façade (d).

Figure 3 Diaphragmatic arches with pyramidal dead weight over vaults.

Figure 4 Deformation at the top of a pier (a), cracks at the base of a pier (b), cracks in a buttress following the perimeter of a false window (c) and deformed flying arches (d).

Figure 5 Observed deformed shapes of the nave transverse sections.

Figure 6 Horizontal displacements (in cm) of the nave transverse sections.

Figure 7 Fourth bay construction stages [29].

Figure 8 Viscoelasticity model: a) schematization through a Maxwell chain and strain (b), stress (c) and stiffness (d) time-dependent laws.

Figure 9 Composite damage surface adopted for masonry.

Figure 10 FE activation technique for sequential analysis: a) all elements inactive (in grey), b) elements corresponding to first construction stage active (in black), c) elements corresponding to second construction stage active and their initial coordinates correction.

Figure 11 Typical bay structure (a) and FE mesh (b) considered for the construction process numerical simulation.

Figure 12 Construction process simulation: first stage (a-b) and second stage (c-d). Deformed shape (x50) with horizontal displacement contour (left) and tensile damage contour (right).

Figure 13 Construction process simulation: horizontal displacement increase at pier top due to creep. Hypotheses of geometric linearity (a) and geometric nonlinearity (b).

Figure 14 Construction process simulation with geometric nonlinearity: a) deformed shape (x50) with horizontal displacement contour (left) and tensile damage (right) for $\xi = 0.875$; b) deformed shape (x10) with horizontal displacement contour (left) and tensile damage (right) for $\xi = 0.975$.

Figure 15 FE mesh adopted for seismic load analysis.

Figure 16 Seismic load multiplier vs. horizontal displacement curves derived from smeared and localized damage models.

Figure 17 Deformed shape and tensile damage obtained by seismic analysis: a) smeared damage model, b) localized damage model with $r_{excl} = 1\,\mathrm{m}$, c) $r_{excl} = 2\,\mathrm{m}$ and d) $r_{excl} = 3\,\mathrm{m}$.

Table 1 Material parameters adopted in numerical analyses.

Structural element	γ (kg/m^3)	E (MPa)	ν (-)	f^+ (MPa)	f^- (MPa)	G_f^+ (J/m^2)	G_f^- (J/m^2)
buttresses, vaults, ribs, clerestory	2100	2000	0.2	0.10	2.00	100	40000
columns, flying arches	2400	8000	0.2	0.40	8.00	100	40000
central vault backing	2000	1000	0.2	0.05	1.00	100	40000

Table 2 Thicknesses of different components in the two-dimensional FE model.

Id.	Structural element	thickness (m)
1	flying arches	0.90
2	clerestory	3.44
3	buttress	1.55
4	column	1.24
5	central vault	1.53
6	lateral clerestory	2.71
7	lateral vault	0.97
8	column/clerestory	2.80

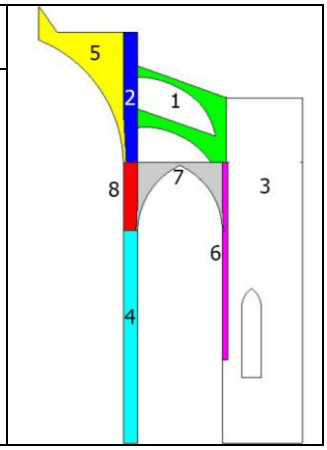

Figure 1

Click here to download high resolution image

Figure 2

Click here to download high resolution image

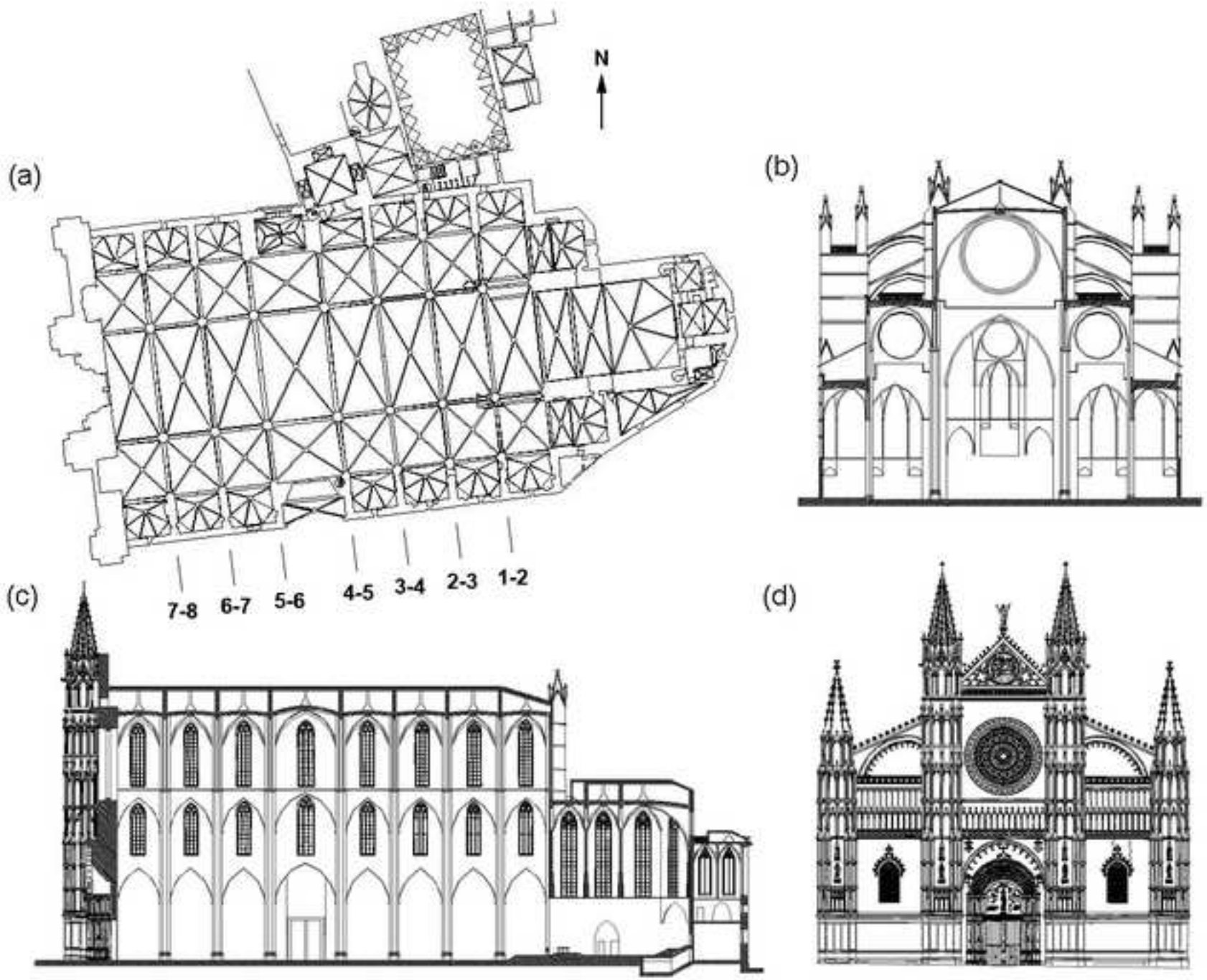

Figure 3

Click here to download high resolution image

Figure 4

Click here to download high resolution image

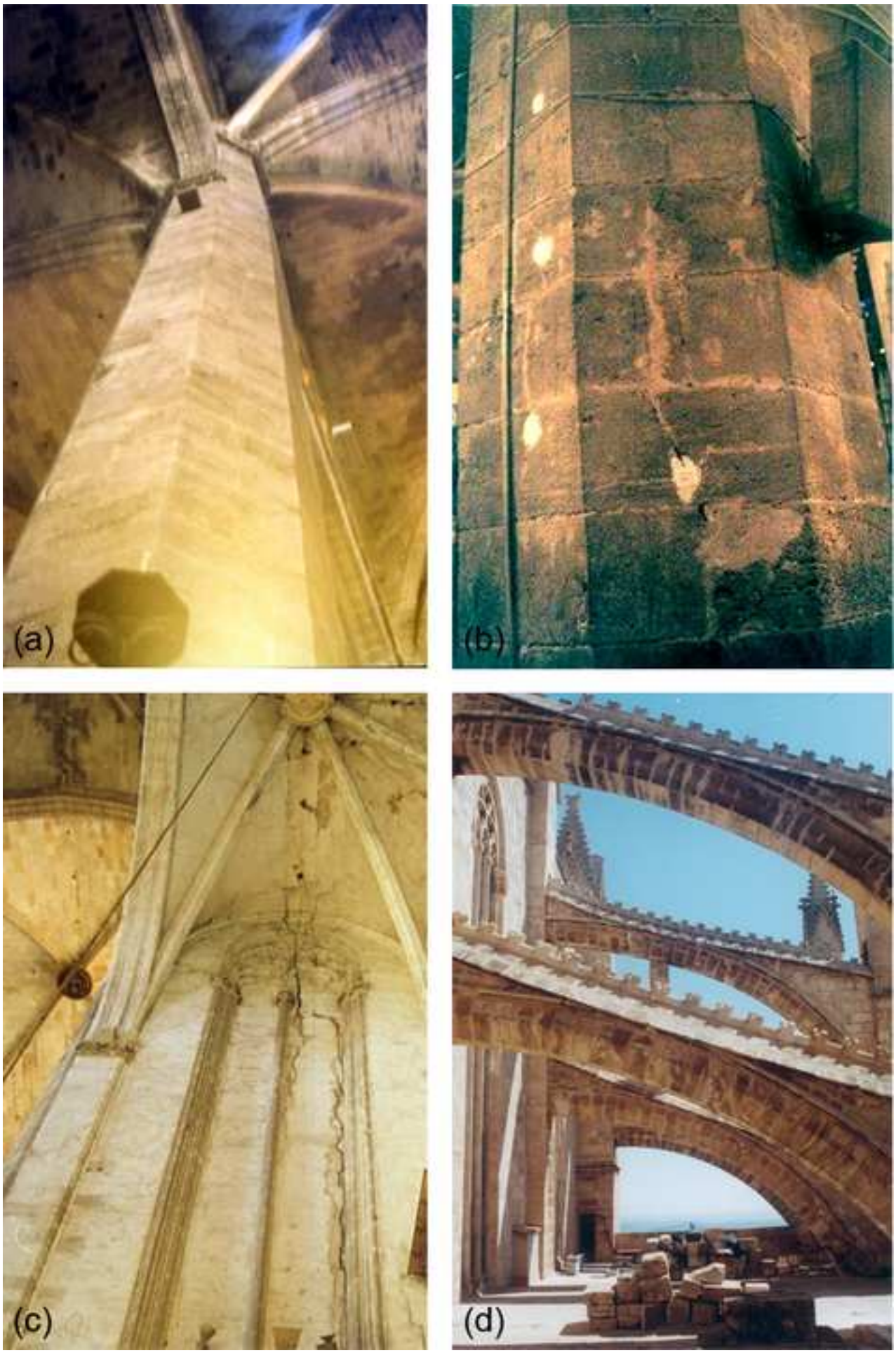

Figure 5

Click here to download high resolution image

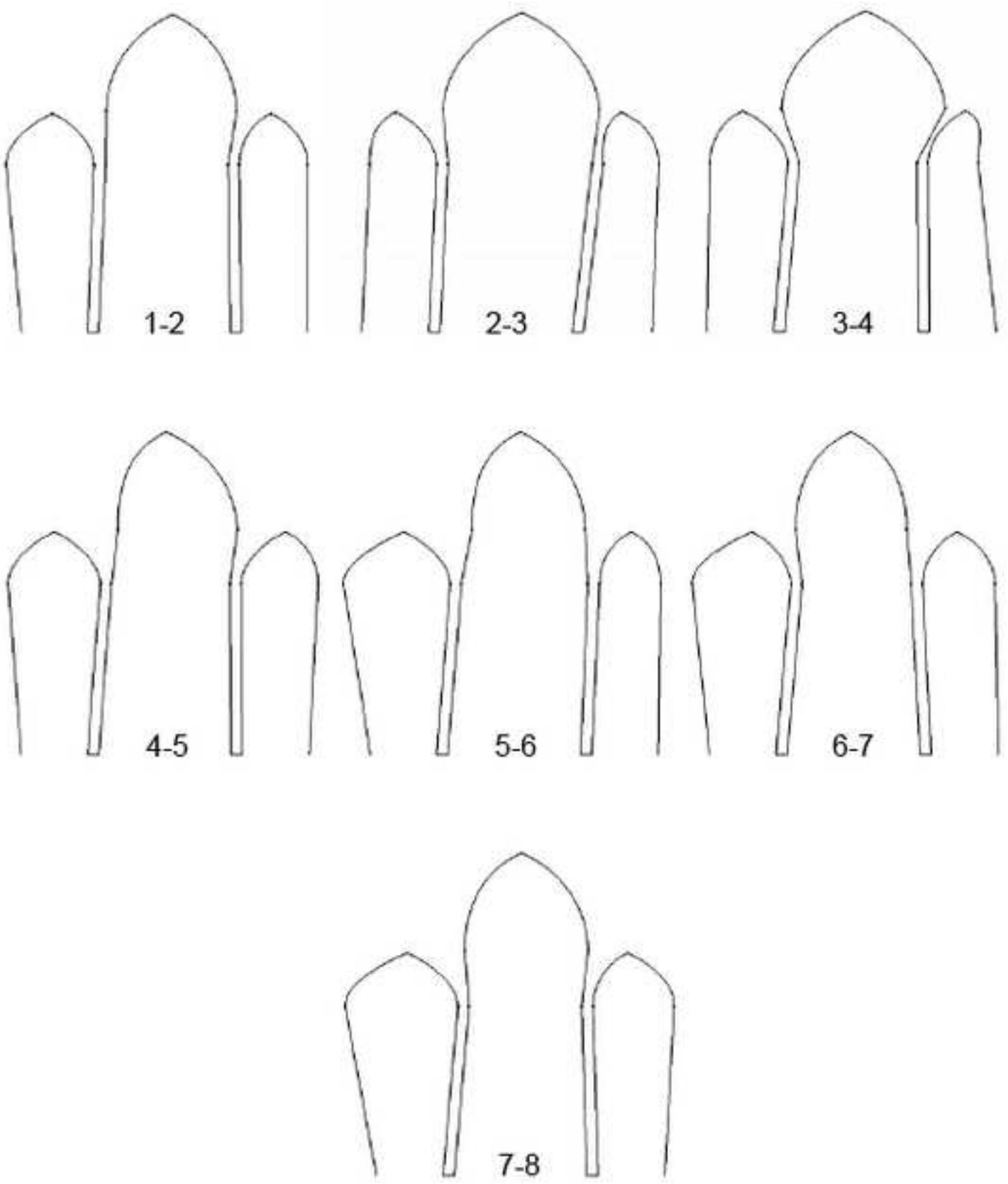

Figure 6

Click here to download high resolution image

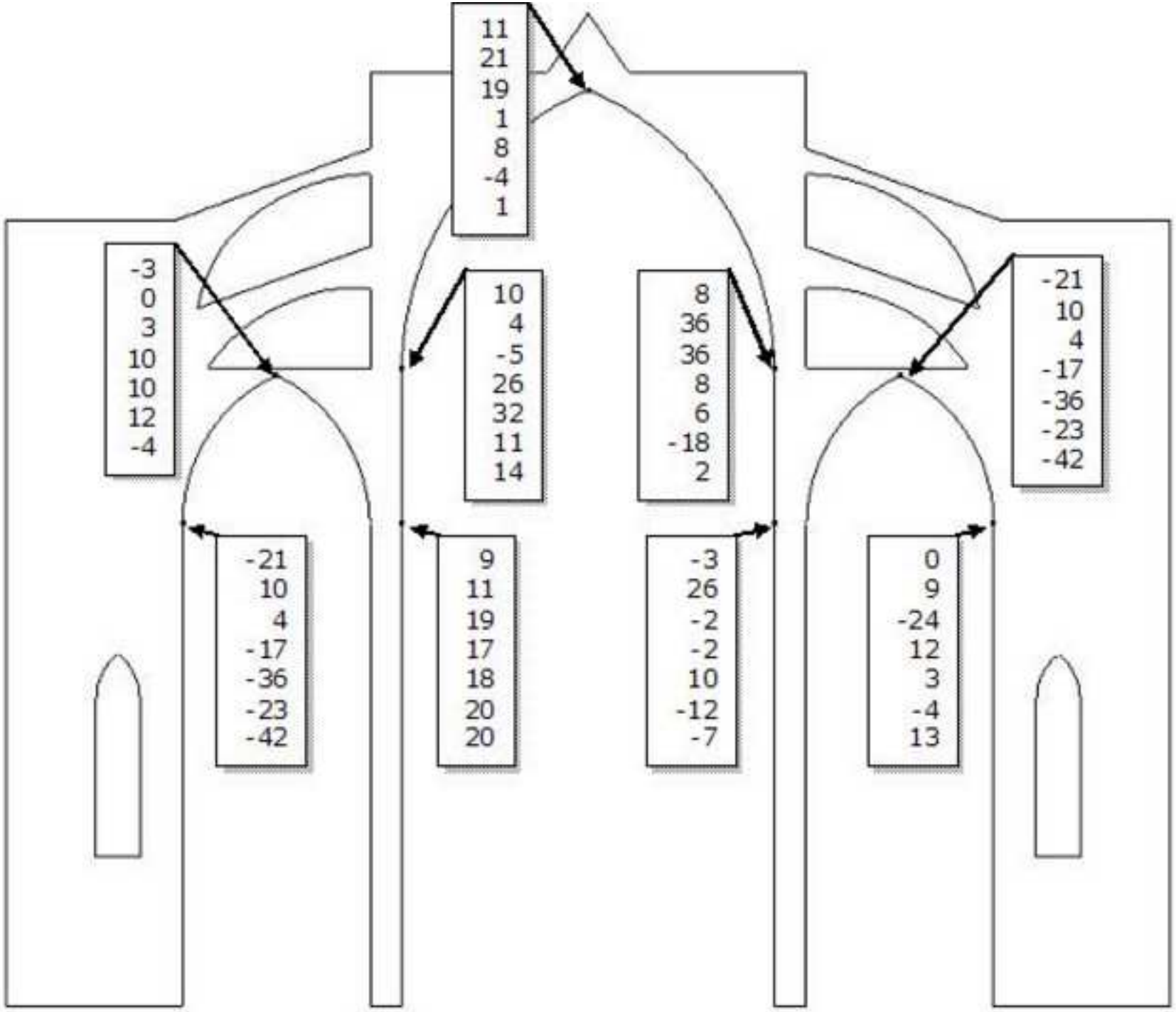

Figure 7
Click here to download high resolution image

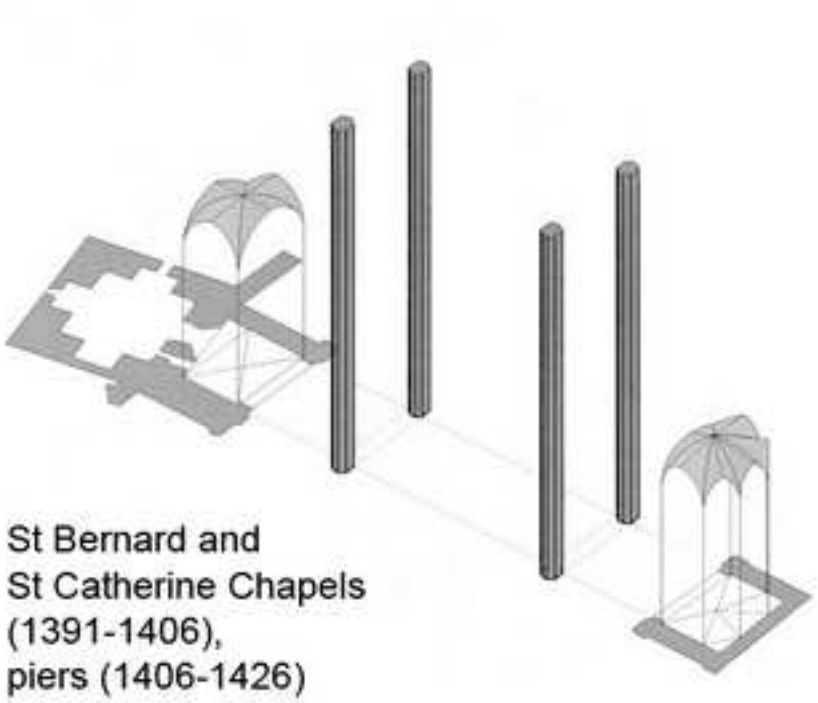

St Bernard and
St Catherine Chapels
(1391-1406),
piers (1406-1426)

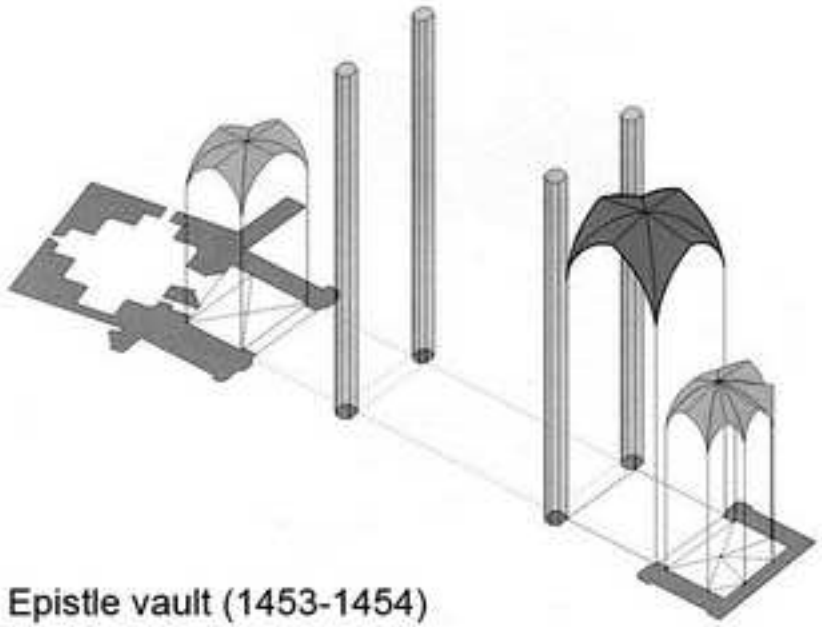

Epistle vault (1453-1454)

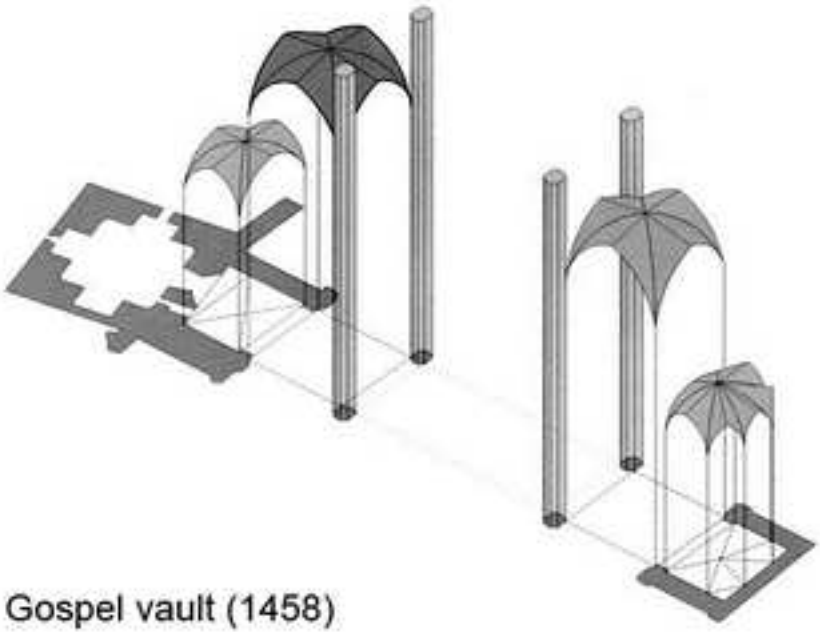

Gospel vault (1458)

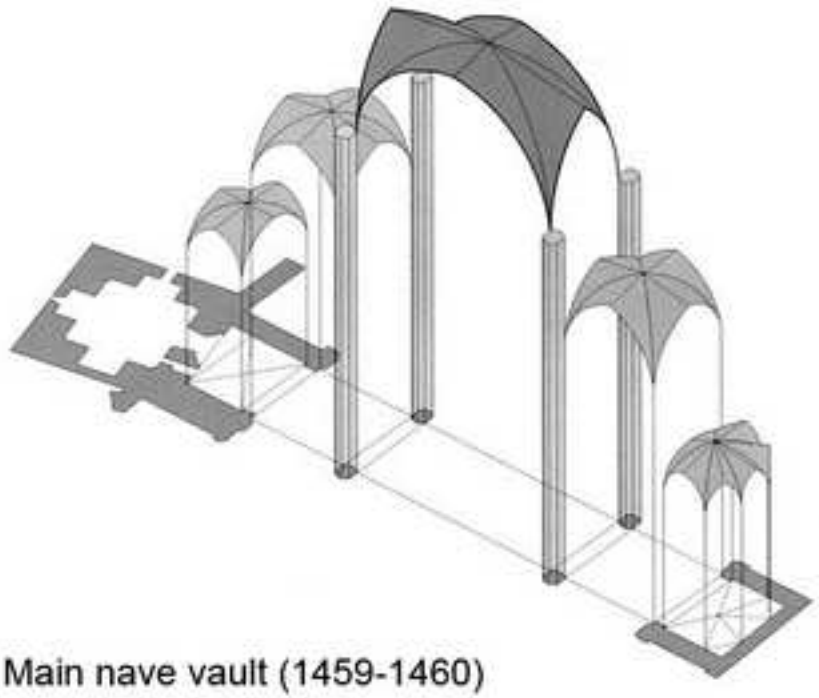

Main nave vault (1459-1460)

Figure 8

Click here to download high resolution image

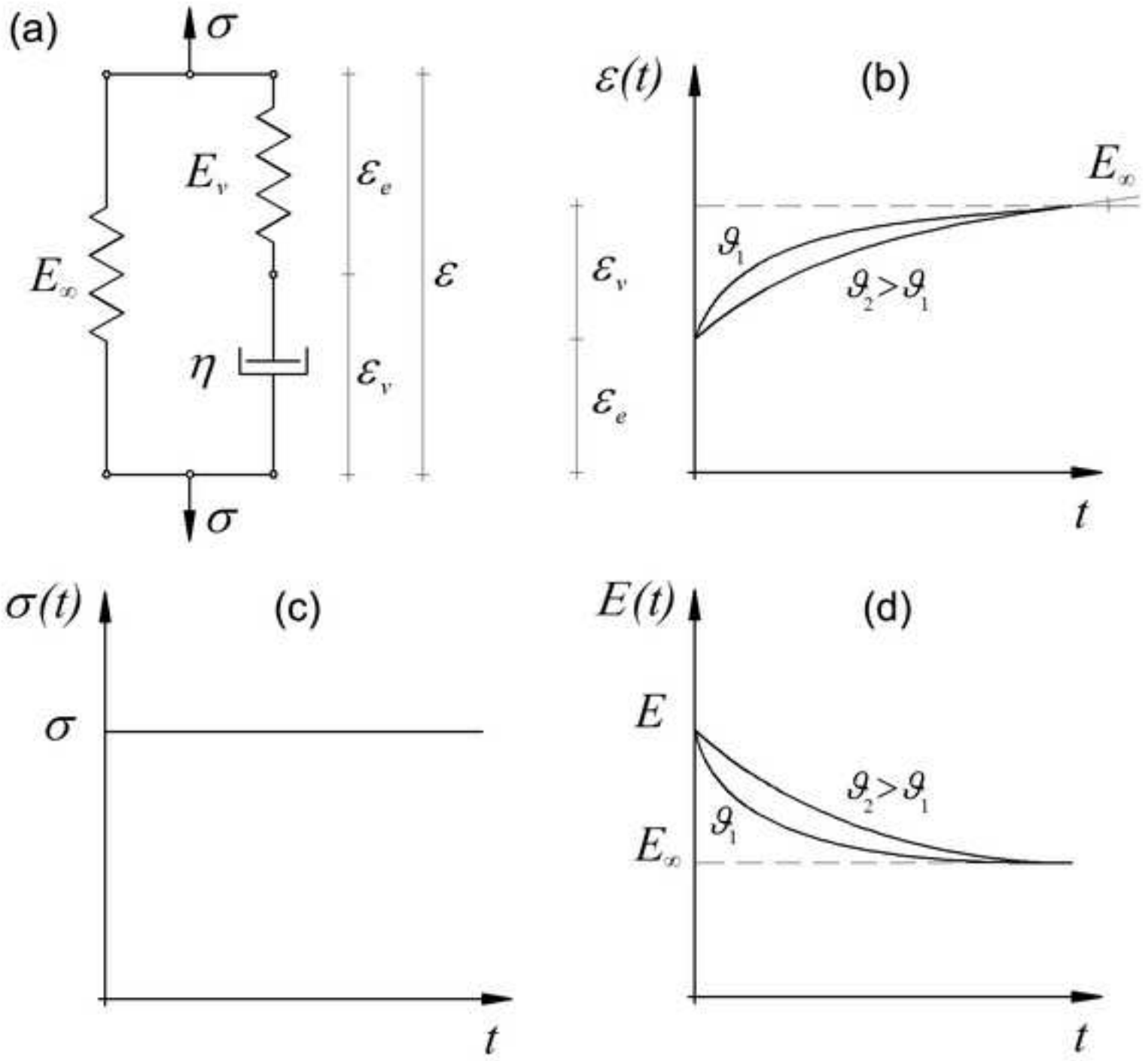

Figure 9

Click here to download high resolution image

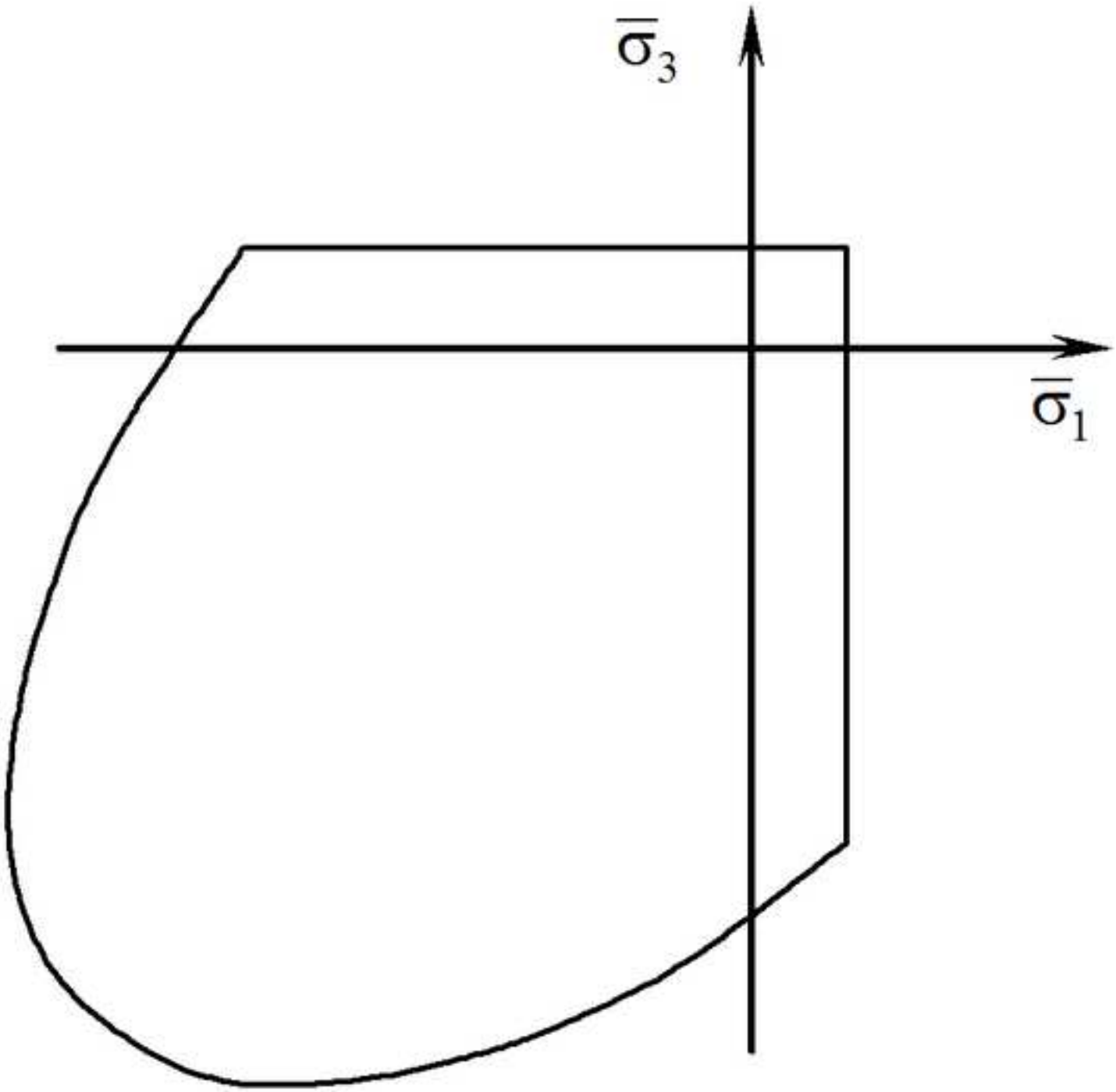

Figure 10

Click here to download high resolution image

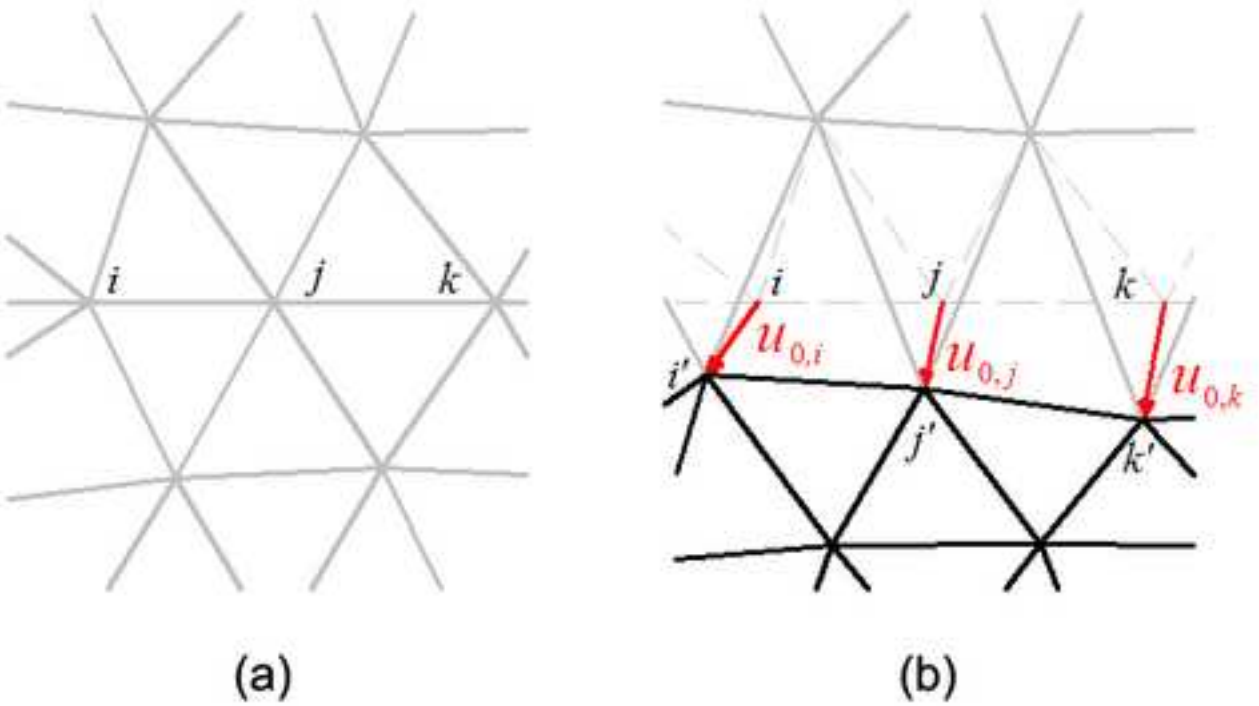

(a) (b) (c)

Figure 11
Click here to download high resolution image

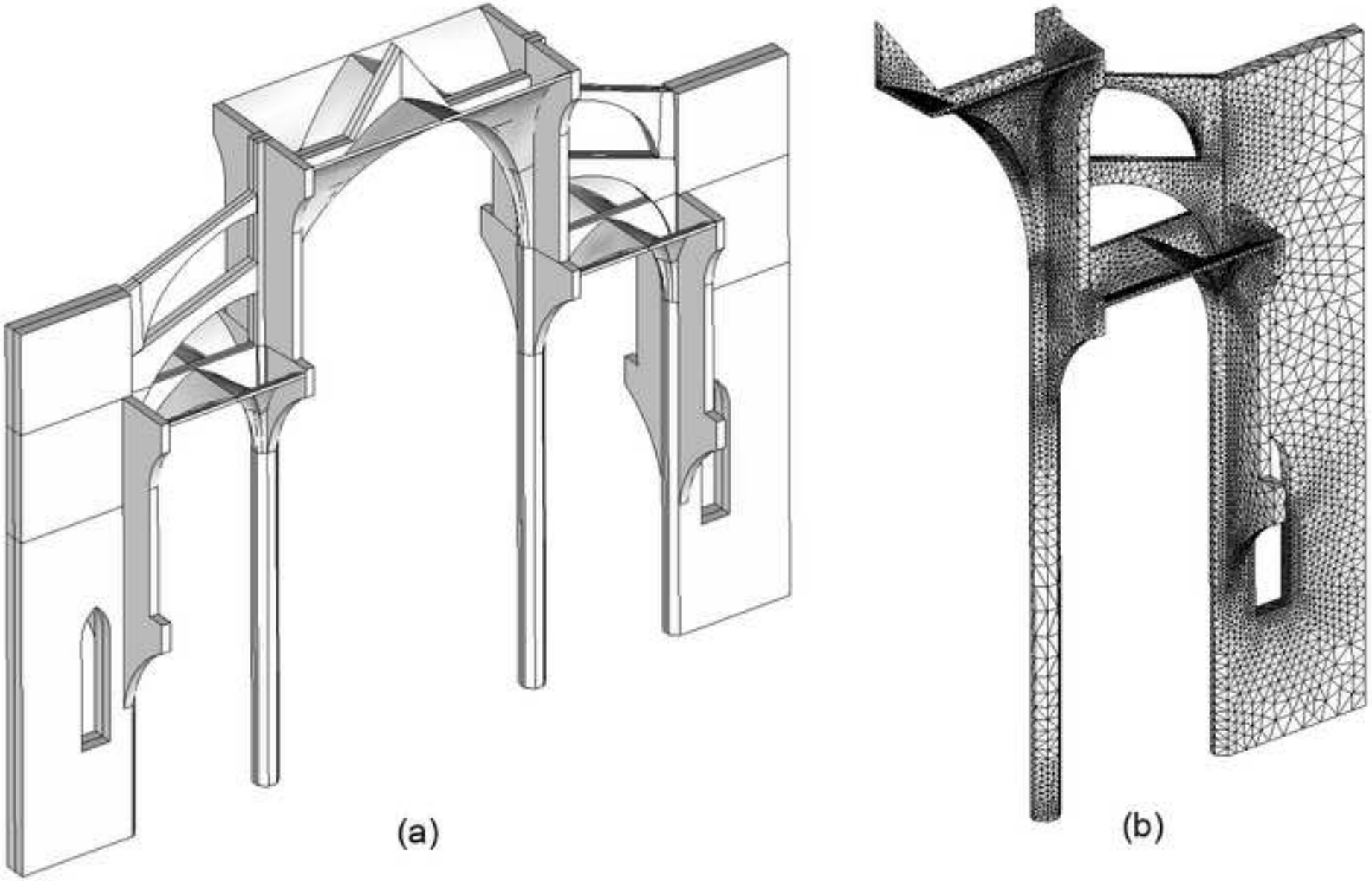

Figure 12

Click here to download high resolution image

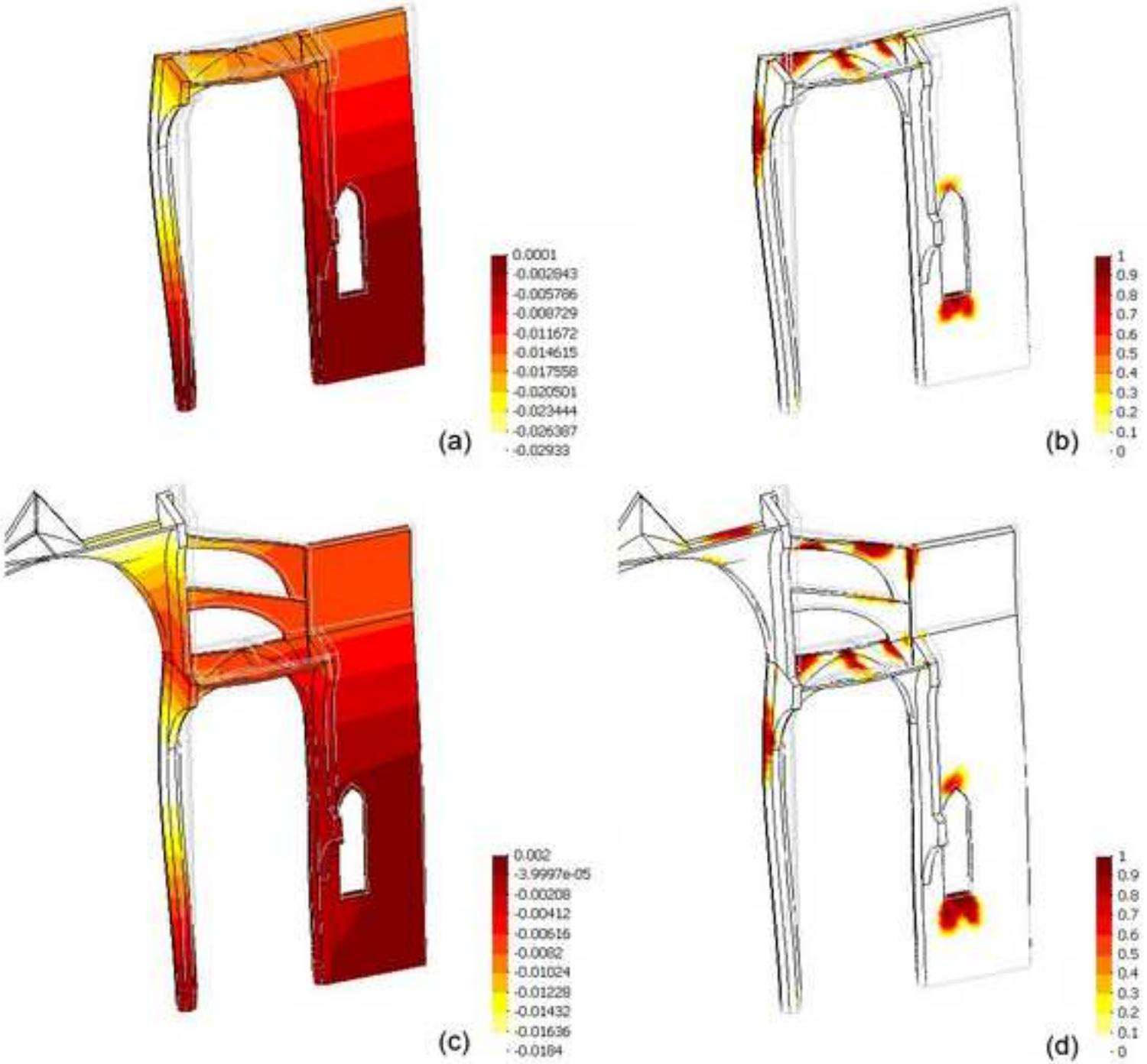

Figure 13
Click here to download high resolution image

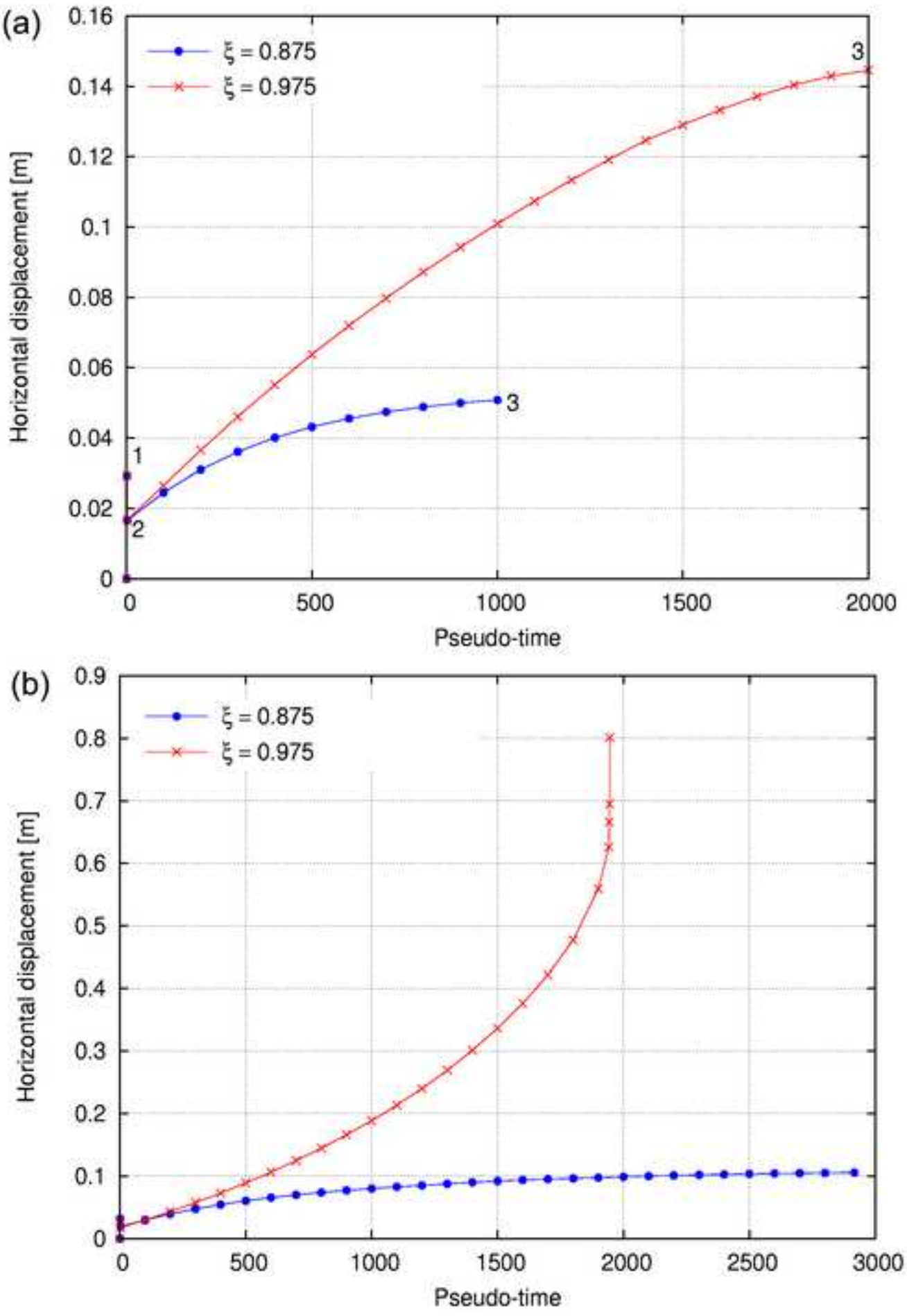

Figure 14

Click here to download high resolution image

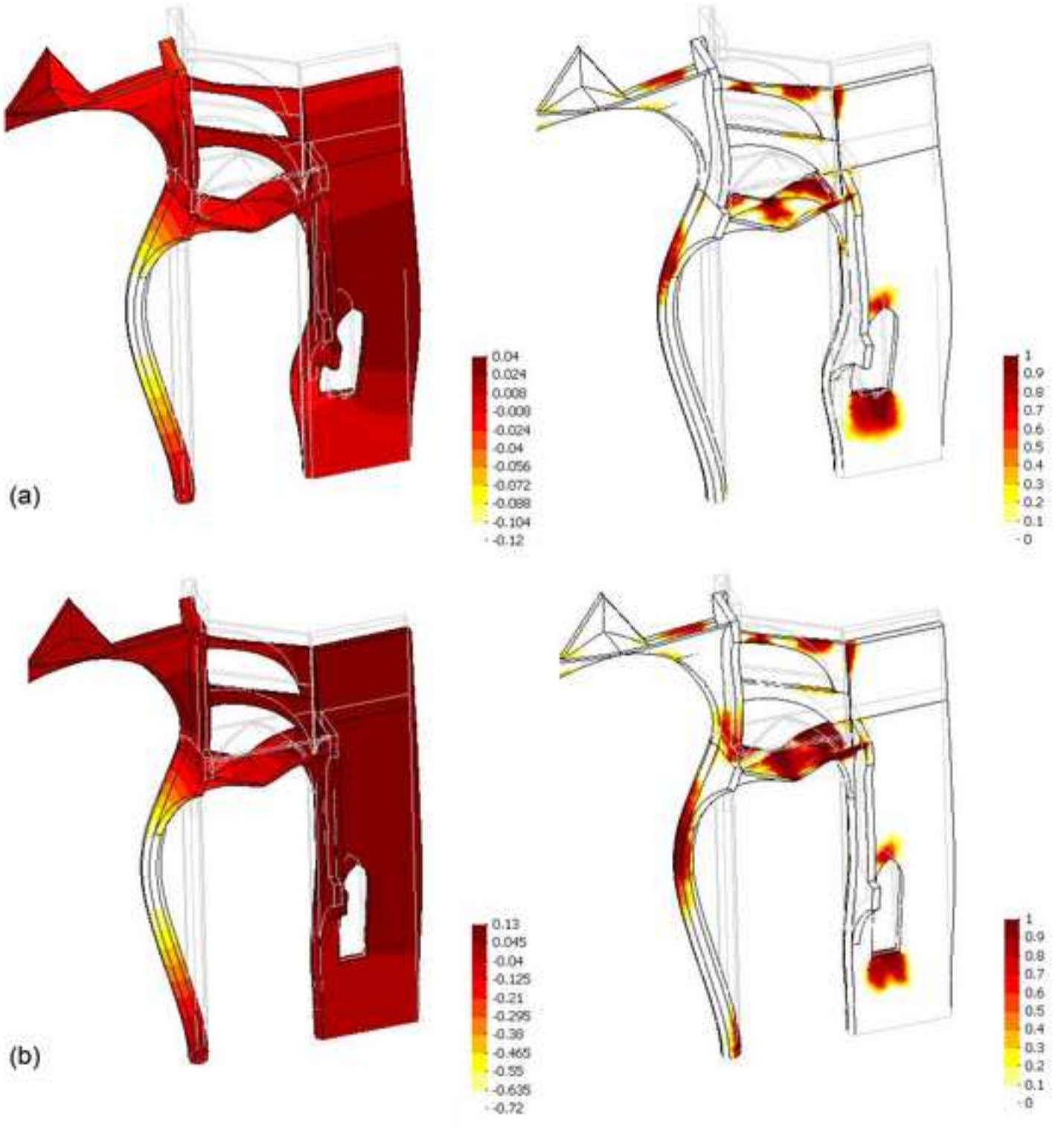

Figure 15

Click here to download high resolution image

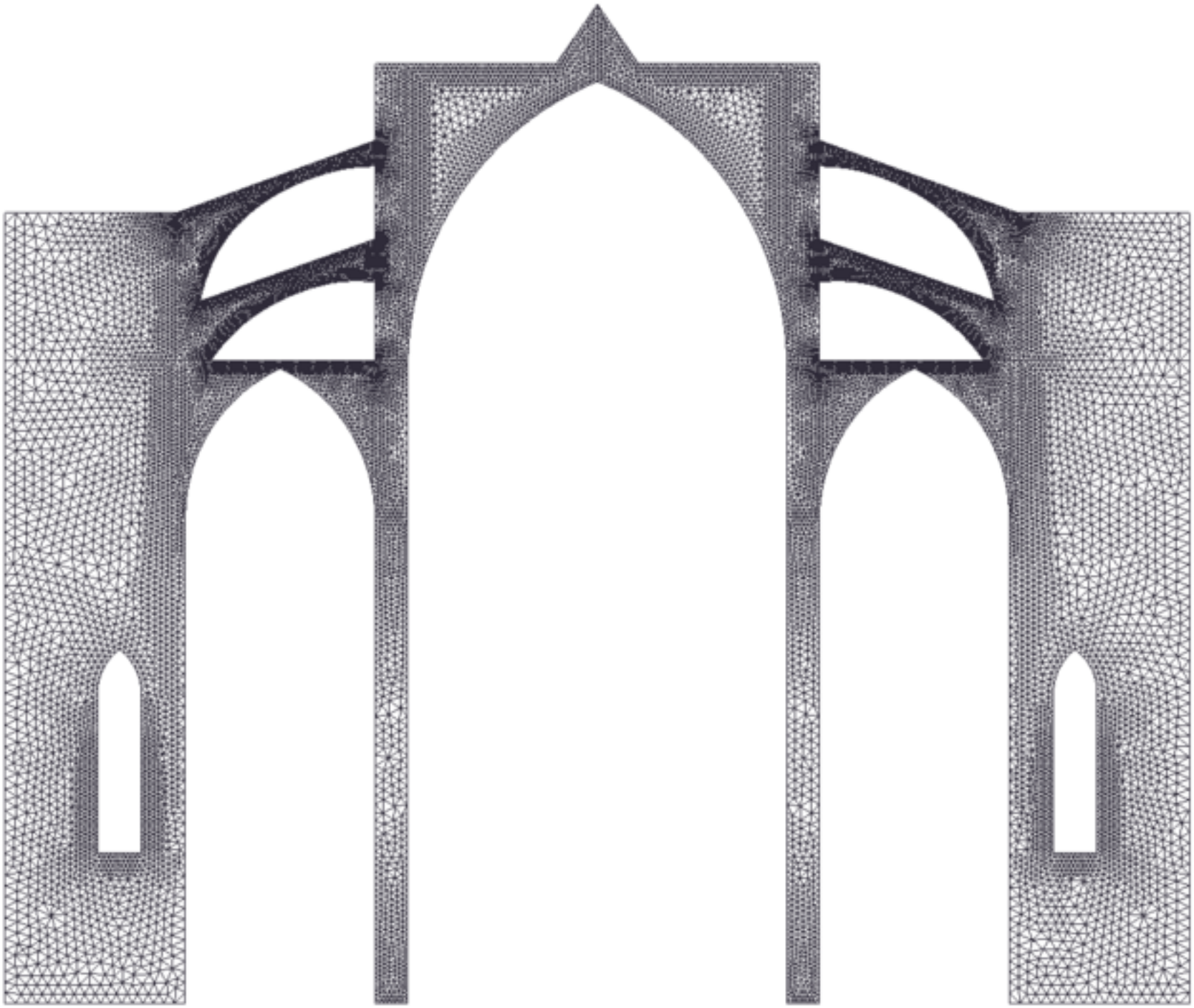

Figure 16
Click here to download high resolution image

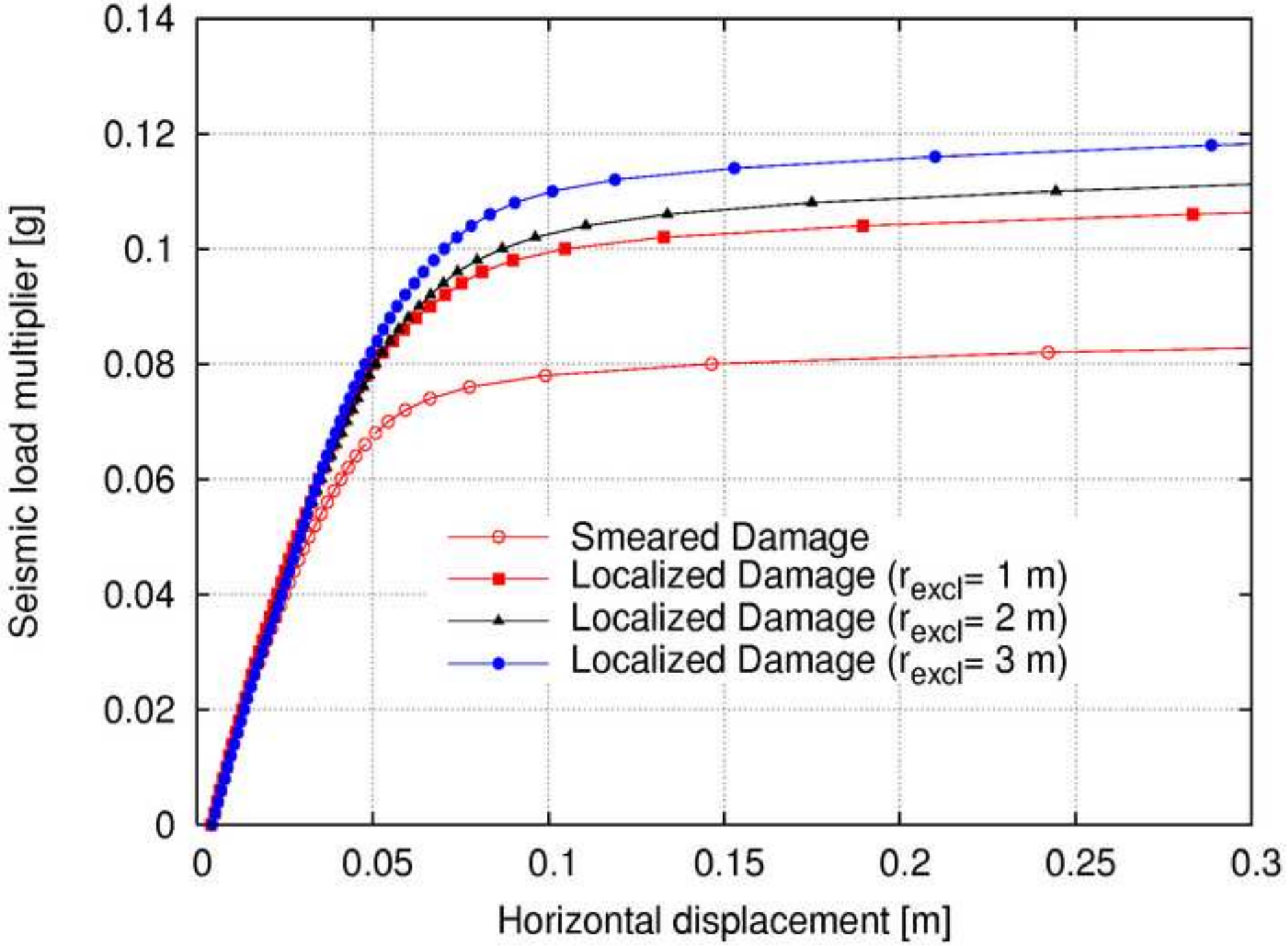

Figure 17

Click here to download high resolution image